

**Hanford Tank Farms Vadose Zone**

**Sixth Recalibration of Spectral Gamma-Ray  
Logging Systems Used for Baseline Characterization  
Measurements in the Hanford Tank Farms**

**C.J. Koizumi**

**August 1999**

Prepared for  
U.S. Department of Energy  
Albuquerque Operations Office  
Grand Junction Office  
Grand Junction, Colorado

Prepared by  
MACTEC-ERS  
Grand Junction Office  
Grand Junction, Colorado

# Contents

	Page
<b>1.0 Overview and Summary of Results</b> .....	1
1.1 Overview .....	1
1.2 General Calibration Function .....	3
1.3 Revised Field Verification Acceptance Criteria .....	4
<b>2.0 Revised Calibration Functions</b> .....	7
2.1 Calibration Standards .....	7
2.2 Data Acquisition .....	9
2.3 Data Analysis .....	9
2.4 Calibration Functions and Recalibration Results .....	12
<b>3.0 Linearity Test Results</b> .....	19
<b>4.0 Comparison of Sixth Recalibration with Previous Recalibrations</b> .....	23
<b>5.0 New Field Verification Criteria</b> .....	27
<b>6.0 Corrections for the 4.5-inch Water-Filled Borehole</b> .....	31
<b>7.0 Acknowledgments</b> .....	47
<b>8.0 References</b> .....	48

## Figures

Figure 2-1. Data and Calibration Function for Gamma 1B .....	17
3-1. Linearity Demonstration for Gamma 1A, 295.2-keV Gamma-Ray Data .....	20
3-2. Linearity Demonstration for Gamma 1B, 609.3-keV Gamma-Ray Data .....	21
3-3. Linearity Demonstration for Gamma 2A, 1764.5-keV Gamma-Ray Data .....	21
3-4. Linearity Demonstration for Gamma 2B, 2204.1-keV Gamma-Ray Data .....	22
6-1. Calculated Water Corrections for Gamma 2A and Gamma 2B .....	34
6-2. Original and Sixth Recalibration Water Corrections for Gamma 2, 4.5-inch Borehole .....	35
6-3. Three Sets of Water Corrections for Gamma 1 .....	37
6-4. Constants A and B for the Water Corrections for Gamma 2A and Gamma 2B ...	38
6-5. Spectrum from the SBM Calibration Standard Recorded by Gamma 1B with Water in the Test Hole .....	39

## Contents (continued)

	Page
Figure 6-6. Spectrum from the KW Calibration Standard Recorded by Gamma 1A with Water in the Test Hole .....	40
6-7. Magnified 609.3-keV Spectral Peaks from Spectrum SBMC005.S0 .....	41
6-8. Magnified 609.3-keV Spectral Peak from Spectrum SBMC005.S0 .....	42
6-9. Magnified 609.3-keV Spectral Peak from Spectrum KW451005.S0 .....	43
6-10. Gamma 1 Water Corrections Calculated with Peaksearch Data Compared to Corrections Calculated with Multifit Data .....	44
6-11. Casing Corrections for Three Casing Thicknesses .....	46

## Tables

Table 1-1. The Four Logging Systems .....	1
1-2. Constants for the General Calibration Function .....	4
1-3. Field Verification Acceptance Criteria for Gamma 1A .....	5
1-4. Field Verification Acceptance Criteria for Gamma 1B .....	6
1-5. Field Verification Acceptance Criteria for Gamma 2A .....	6
1-6. Field Verification Acceptance Criteria for Gamma 2B .....	6
2-1. Calibration Standard Source Concentrations .....	7
2-2. Reference Standards for Calibration Source Concentrations .....	7
2-3. PCMCA/WIN Comparison of SBK Data .....	10
2-4. PCMCA/WIN Comparison of SBM Data .....	11
2-5. Weighted Average Spectral Peak Intensities for Gamma 1A .....	13
2-6. Weighted Average Spectral Peak Intensities for Gamma 1B .....	14
2-7. Weighted Average Spectral Peak Intensities for Gamma 2B .....	15
2-8. Weighted Average Spectral Peak Intensities for Gamma 2B .....	16
3-1. Factors for the Dead Time Correction .....	19
4-1. Calibration and Recalibration Constants for Gamma 1A and Gamma 1B .....	23
4-2. Calibration and Recalibration Constants for Gamma 2A and Gamma 2B .....	23
4-3. Details of Three Hypothetical Gamma-Ray Sources .....	24
4-4. Hypothetical Concentrations Illustrating Performances of Logging Systems over Time .....	25
5-1. Outcomes of Field Verification Measurements .....	28
5-2. Outcomes of Field Verification Measurements Involving Followup Spectra .....	29
6-1. Corrections for Gamma 1A and Gamma 1B .....	32
6-2. Corrections for Gamma 2A and Gamma 2B .....	33
6-3. Constants A and B for the Water Corrections for Gamma 2A and Gamma 2B .....	35
6-4. Gamma 2 Water Corrections for Gamma Rays of Primary Importance .....	36

## Hanford Tank Farms Vadose Zone

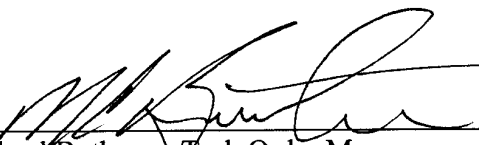
### Sixth Recalibration of Spectral Gamma-Ray Logging Systems Used for Baseline Characterization Measurements in the Hanford Tank Farms

Prepared by:

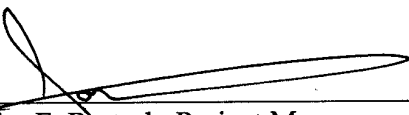
  
\_\_\_\_\_  
Carl J. Koizumi, Technical Lead  
MACTEC-ERS, Grand Junction Office

8/5/99  
\_\_\_\_\_  
Date

Approved by:

  
\_\_\_\_\_  
Michael Butherus, Task Order Manager  
MACTEC-ERS, Grand Junction Office

8/3/99  
\_\_\_\_\_  
Date

  
\_\_\_\_\_  
Jim F. Bertsch, Project Manager  
MACTEC-ERS, Hanford Office

8/3/99  
\_\_\_\_\_  
Date

# 1.0 Overview and Summary of Results

## 1.1 Overview

The U.S. Department of Energy (DOE) Richland Operations Office (DOE-RL) enlisted the DOE Grand Junction Office (DOE-GJO) to develop a baseline characterization of the gamma-ray-emitting radionuclides that are constituents of the radioactive waste that exists in the vadose zone sediments beneath and around the single-shell tanks (SSTs) at the Hanford Site. The baseline data are acquired by logging existing monitoring boreholes with high-resolution passive spectral gamma-ray logging systems (SGLSs). Analyses of the recorded spectra yield the pulse heights and intensities of the full energy spectral peaks (peaks). From the pulse heights, the gamma-ray energies are determined, and these energies are the basis for unambiguous identifications of the gamma-ray source nuclides. The peak intensities are used to calculate the concentrations of the source nuclides in the media surrounding the boreholes. These concentration calculations employ the logging system calibration functions.

The acquisition of baseline characterization data began in 1995 with the deployment of two SGLSs, each consisting of a surface support system (vehicle, logging cable control system, data acquisition system electronics) and a sonde. In 1997 a third sonde was acquired. In routine operations, the original sondes are never exchanged between logging systems, but the third sonde is used as a backup component to either logging system. Thus, the two surface support systems and three sondes can be utilized in the four configurations displayed in Table 1-1.

*Table 1-1. The Four Logging Systems*

Surface Support System	Sonde	Logging System Name
Gamma 1 DOE Vehicle Number HO68B3572	Original Detector Serial Number 34TP20893A	Gamma 1 or Gamma 1A
	Backup Detector Serial Number 36TP21095A	Gamma 1B
Gamma 2 DOE Vehicle Number HO68B3574	Original Detector Serial Number 34TP11019B	Gamma 2 or Gamma 2A
	Backup Detector Serial Number 36TP21095A	Gamma 2B

Periodic recalibration of the SGLSs, as prescribed by the project document *Vadose Zone Monitoring Project at the Hanford Tank Farms, Spectral Gamma-Ray Borehole Geophysical Logging Characterization and Baseline Monitoring Plan for the Hanford Single-Shell Tanks* (DOE 1995a), ensures that the radionuclide concentrations derived from the log data are defensibly linked to DOE calibration standards. The (original) logging systems were calibrated at the beginning of the

characterization project. Those initial, or base, calibrations utilized the borehole gamma-ray calibration standards at the DOE Grand Junction Office, and the measurements and results are documented in DOE (1995b). Subsequent recalibrations utilized the calibration standards at the Hanford borehole logging calibration center and were performed biannually. The first, second, third, fourth, and fifth biannual recalibrations are described in DOE (1996a, 1996b, 1997, 1998a, and 1998b), respectively.

Following the acquisition of data for the fifth biannual recalibrations in October 1997, MACTEC-ERS technical staff members evaluated all of the calibration and field verification data and determined that the stability of each logging system over time justified a change in the recalibration schedule from biannual to annual. Thus, the data for the sixth recalibration were acquired in the fall of 1998. From analyses of these data the following were accomplished:

- C The factors in the general calibration functions for natural and man-made gamma-ray sources were revised. The changes in the calibration functions resulting from these revisions were minor. Thus, the logging systems continued to exhibit the stability that was consistently observed during the previous recalibrations.
- C Linearity of logging system response in relation to source intensity was reconfirmed for each logging system over a range of source intensities exceeding the range spanned by the sources in the calibration standards. These linearity demonstrations validate the system dead time corrections.
- C The sixth recalibration results were compared to results from previous calibrations and recalibrations, and no significant changes were observed.
- C During logging operations, the performance of each logging system is frequently checked by recording spectra with a standard source (*Amersham KUTh Field Verifier*), then confirming that the intensities and full widths at half maxima (FWHM) of selected spectral peaks fall within acceptable ranges. These parameter ranges, or field verification acceptance criteria, are reviewed and revised at each recalibration. For the sixth recalibration, the verification method and the verification criteria were revamped.
- C Data were recorded for determination of corrections for water-filled 4.5-inch-diameter boreholes. These corrections were established for Gamma 1A and Gamma 2A from measurements taken at the base calibrations (DOE 1995b), but corrections for water-filled boreholes were never directly established for Gamma 1B or Gamma 2B. When corrections were required, data acquired with Gamma 1B and Gamma 2B were corrected with the corrections for Gamma 1A and Gamma 2A, respectively. The new water corrections were derived to justify this practice, and also to fortify the contention that environmental corrections are stable over time. The results for Gamma 2A and Gamma 2B conform to expectations, but the results for Gamma 1A and Gamma 1B indicate that the Gamma 1A corrections are incorrect. Analyses of the original and new corrections indicate that the original water corrections for Gamma 1A should be abandoned, and data taken from water-filled boreholes with Gamma 1A or Gamma 1B should be corrected with the corrections for Gamma 2A.

All of the earlier calibration and recalibration reports presented calibrations that were specific to potassium, radium, and thorium. Examples of these source-specific calibrations are provided by Equation 1-1 and Tables 1-2 through 1-5 in DOE (1998b). However, the method represented by Equation 1-1 in DOE (1998b) has never been used to analyze project data, so the potassium, radium, and thorium calibrations are not included in this report.

The new calibration factors and field verification acceptance criteria are presented in Table 1-2 and Tables 1-3 through 1-6 in Sections 1.2 and 1.3, respectively, for the data analysts' convenient reference.

Later sections in this report give details about the calibration data, data analyses, stabilities of system performances over time, and water-filled borehole corrections. Section 2.2 describes data acquisition, and Section 2.3 summarizes the data processing that produced the revised calibration factors. Comparisons of representative new calibration results with those of prior calibrations appear in Section 4.0. The comparisons show that the efficiencies of the logging systems have fluctuated over time, but the variations have been minor and the system performances can be regarded to have been stable since commencement of logging for the characterization project.

## **1.2 General Calibration Function**

The SGLS calibration is formulated in terms of an energy-dependent calibration function that is defined as the ratio of the gamma-ray source intensity to the intensity of the associated peak in the gamma-ray spectrum. Thus, the value of the function at a particular gamma-ray energy can be determined by the following straightforward method. The source intensity (in gammas per second per gram) for a particular gamma ray and a particular calibration standard is calculated from the source concentration (in picocuries per gram) and gamma-ray yield (in gammas per decay). The calibration standard is logged to obtain a gamma-ray spectrum, and the spectrum is analyzed to determine the intensity (in counts per second) of the spectral peak associated with the particular gamma ray. The value of the calibration function is then calculated by dividing the source intensity by the spectral peak intensity.

The calibration standards contain potassium, radium (uranium), and thorium gamma-ray sources that provide gamma rays with energies ranging from about 130 keV to 2614.5 keV. Spectral peaks for these gamma rays are used, along with the source intensities, to determine values of the calibration function for a number of discrete gamma-ray energies.

After values of the calibration function are calculated for several discrete gamma-ray energies, a curve fitting program is employed to obtain an analytical function that expresses the relationship of source intensity to spectral peak intensity. This function is the general calibration function.

After the function is determined, the intensity of any gamma-emitting source surrounding a borehole can be calculated by logging the borehole to record a spectrum, calculating the intensity of the appropriate

peak in the spectrum, and multiplying the peak intensity by the value of the calibration function for the particular energy. The source concentration is easily calculated from the source intensity.

The general SGLS calibration function is

$$I(E) = (C + D \ln(E))^2. \quad (1-1)$$

This calibration function is used for all gamma-ray sources, natural or man-made. The accuracy of a gamma-ray source concentration calculated with this function depends on several factors, the most important of which may be the distribution of the source in the subsurface. Every calibration spectrum was collected with the detector surrounded by a large homogeneous volume of source-bearing material, so the calibration results are optimized to this source-detector configuration. Source concentrations calculated from field data will therefore be most accurate when the gamma-ray sources in the subsurface are similarly distributed.

At each recalibration, the constants  $C$  and  $D$  in Equation (1-1) are recalculated using data recorded by logging the calibration standards. Table 1-2 displays the new values for  $C$  and  $D$ . These values are appropriate if  $E$  is in kilo-electron-volt units and  $I(E)$  is expressed in gammas per second per gram per count per second.

*Table 1-2. Constants for the General Calibration Function*

Logging System	$C \pm 2s C^1$	$D \pm 2s D$	Effective Dates
Gamma 1A	$0.0195 \pm 0.0036$	$0.01524 \pm 0.00054$	08/12/1998
Gamma 1B	$0.0277 \pm 0.0041$	$0.01394 \pm 0.00061$	09/08/1998
Gamma 2A	$0.0093 \pm 0.0053$	$0.01846 \pm 0.00080$	10/01/1998
Gamma 2B	$0.0242 \pm 0.0057$	$0.01433 \pm 0.00086$	09/24/1998

<sup>1</sup> The notation “ $2s C$ ” denotes the two-sigma uncertainty in  $C$ .

### 1.3 Revised Field Verification Acceptance Criteria

A logging run produces a set of borehole measurements recorded sequentially in depth and time with the data acquisition parameters held constant. The logging of a borehole may require one or several logging runs. In routine operations, at least one field verification spectrum is recorded before each logging run, and at least one additional spectrum is recorded upon completion of the run. The gamma-ray sources for field verification are Amersham *KUTH Field Verifier* sources.

In the past, proper operation of the logging system was ascertained if the intensities and full widths at half maxima (FWHM) of selected spectral peaks in a field verification spectrum fell within ranges defined by upper and lower acceptance tolerances. If the field verification spectra produced an



occasional FWHM or peak intensity that was outside of the tolerances, no action was taken, but if readings outside of the ranges were consistently recorded, field measurements were suspended until the logging system could be checked for equipment malfunctions.

Before the sixth recalibration, acceptance tolerances were derived and used by methods described in Section 4.0 of DOE (1998b). Because of the demonstrated stability of system performance over time, those methods have now been replaced with a two-tier acceptance test based on conventional control chart practice. Both peak intensity and FWHM for the three spectral peaks associated with the 609.3-keV, 1460.8-keV, and 2614.5-keV gamma rays are compared to warning and control limits derived from the two-sigma and three-sigma deviations from the mean value. A logging system passes the acceptance test if all six of the parameters (three peak intensities and three FWHM) of a field verification spectrum lie within corresponding warning limits. If one of the six parameter values falls outside of the warning limits for the parameter, the next verification spectrum is examined, and if the same parameter value also falls outside the warning limits, on the same side of the limit range as the first discrepancy, the acceptance test is failed. If the same parameter value falls outside the warning limits, but on the opposite side of the limit range, then a third spectrum must be examined. If the same parameter from the third spectrum also lies outside the warning limit, then the acceptance test is failed.

A logging system malfunction is assumed if a field verification reading falls outside the control limits. In other words, if any FWHM or peak intensity value lies outside of the control limits, the logging system fails the acceptance test.

Warning and control limits for the four logging systems are listed in Tables 1-3, 1-4, 1-5, and 1-6. These acceptance criteria are applicable until new acceptance criteria are established by the next recalibration.

Derivations of these criteria are described in Section 5.0.

*Table 1-3. Field Verification Acceptance Criteria for Gamma 1A<sup>1</sup>*

Gamma-Ray Energy (keV)	Parameter	Warning Limits		Control Limits	
		Lower	Upper	Lower	Upper
609.3	Peak intensity	8.86 c/s	10.07 c/s	8.56 c/s	10.37 c/s
	FWHM	1.82 KeV	2.52 KeV	1.65 KeV	2.69 KeV
1460.8	Peak intensity	9.83 c/s	11.24 c/s	9.48 c/s	11.59 c/s
	FWHM	2.18 KeV	2.76 KeV	2.04 KeV	2.90 KeV
2614.5	Peak intensity	2.12 c/s	2.51 c/s	2.02 c/s	2.61 c/s
	FWHM	2.59 KeV	3.36 KeV	2.40 KeV	3.55 KeV

<sup>1</sup> These criteria are applicable between January 23, 1998 and the establishment of new criteria at the seventh recalibration.

*Table 1-4. Field Verification Acceptance Criteria for Gamma 1B <sup>1</sup>*

Gamma-Ray Energy (keV)	Parameter	Warning Limits		Control Limits	
		Lower	Upper	Lower	Upper
609.3	Peak intensity	8.68 c/s	9.99 c/s	8.35 c/s	10.32 c/s
	FWHM	1.92 KeV	2.13 KeV	1.86 KeV	2.19 KeV
1460.8	Peak intensity	9.98 c/s	11.50 c/s	9.60 c/s	11.88 c/s
	FWHM	2.24 KeV	2.52 KeV	2.17 KeV	2.58 KeV
2614.5	Peak intensity	2.19 c/s	2.57 c/s	2.09 c/s	2.66 c/s
	FWHM	2.68 KeV	3.17 KeV	2.56 KeV	3.29 KeV

<sup>1</sup> These criteria are applicable between May 20, 1998 and the establishment of new criteria at the seventh recalibration.

*Table 1-5. Field Verification Acceptance Criteria for Gamma 2A <sup>1</sup>*

Gamma-Ray Energy (keV)	Parameter	Warning Limits		Control Limits	
		Lower	Upper	Lower	Upper
609.3	Peak intensity	7.55 c/s	8.96 c/s	7.20 c/s	9.31 c/s
	FWHM	1.67 KeV	1.85 KeV	1.63 KeV	1.90 KeV
1460.8	Peak intensity	8.57 c/s	10.04 c/s	8.21 c/s	10.41 c/s
	FWHM	2.08 KeV	2.37 KeV	2.01 KeV	2.44 KeV
2614.5	Peak intensity	1.79 c/s	2.18 c/s	1.69 c/s	2.28 c/s
	FWHM	2.48 KeV	3.15 KeV	2.32 KeV	3.32 KeV

<sup>1</sup> These criteria are applicable between September 22, 1998 and the establishment of new criteria at the seventh recalibration.

*Table 1-6. Field Verification Acceptance Criteria for Gamma 2B <sup>1</sup>*

Gamma-Ray Energy (keV)	Parameter	Warning Limits		Control Limits	
		Lower	Upper	Lower	Upper
609.3	Peak intensity	8.58 c/s	9.90 c/s	8.26 c/s	10.22 c/s
	FWHM	1.71 KeV	1.84 KeV	1.68 KeV	1.87 KeV
1460.8	Peak intensity	10.20 c/s	11.69 c/s	9.83 c/s	12.06 c/s
	FWHM	2.12 KeV	2.31 KeV	2.07 KeV	2.36 KeV
2614.5	Peak intensity	2.20 c/s	2.58 c/s	2.10 c/s	2.68 c/s
	FWHM	2.53 KeV	3.02 KeV	2.41 KeV	3.14 KeV

<sup>1</sup> These criteria are applicable between March 12, 1999 and the establishment of new criteria at the seventh recalibration.

## 2.0 Revised Calibration Functions

### 2.1 Calibration Standards

The Hanford borehole calibration standards and their links to New-Brunswick-Laboratory-certified standards, and other standards, are described in Heistand et al. (1984) and Leino et al. (1994). The names of the borehole standards and their source “concentrations” (actually, decay rates per unit mass) are displayed in Table 2-1.

*Table 2-1. Calibration Standard Source Concentrations*

Standard	<sup>40</sup> K Concentration (pCi/g)	<sup>226</sup> Ra Concentration <sup>1</sup> (pCi/g)	<sup>232</sup> Th Concentration (pCi/g)
<b>SBK</b> <sup>2,3</sup>	53.50 ± 1.67	1.16 ± 0.11	0.11 ± 0.02
<b>SBU</b> <sup>2,3</sup>	10.72 ± 0.84	190.52 ± 5.81	0.66 ± 0.06
<b>SBT</b> <sup>2,3</sup>	10.63 ± 1.34	10.02 ± 0.48	58.11 ± 1.44
<b>SBM</b> <sup>2,3</sup>	41.78 ± 1.84	125.79 ± 4.00	39.12 ± 1.07
<b>SBA</b> <sup>3</sup>	undetermined	61.2 ± 1.7	undetermined
<b>SBL</b> <sup>3</sup>	undetermined	324 ± 9	undetermined
<b>SBB</b> <sup>3</sup>	undetermined	902 ± 27	undetermined

<sup>1</sup> If <sup>226</sup>Ra is in decay equilibrium with <sup>238</sup>U, then the concentrations (decay rates) of the two nuclides are equal.

<sup>2</sup> Standards used for calibration.

<sup>3</sup> Standards used for linearity checks.

Table 2-2 lists the gamma-ray counting standards to which the source concentrations in the borehole standards are referenced.

*Table 2-2. Reference Standards for Calibration Source Concentrations*

Source	Reference Standard
Potassium ( <sup>40</sup> K)	Reagent-grade potassium carbonate (K <sub>2</sub> CO <sub>3</sub> )
Radium ( <sup>226</sup> Ra)	NBL (New Brunswick Laboratory) 100-A Series Uranium <sup>1</sup>
Thorium ( <sup>232</sup> Th)	NBL 100-A Series Thorium <sup>1</sup>

<sup>1</sup> Trahey et al. (1982).

Previous recalibration reports, e.g., DOE (1998b), acknowledged that the pores in the calibration standard materials contain unknown concentrations of water, but the source concentrations are reported in terms of decay activity *per unit dry mass* (Leino et al. 1994). This means that the data used to calculate the constants *C* and *D* in the calibration equation (Equation 1-1) consist of *concentrations based on dry mass and spectral peak intensities from water-bearing standards*. If the subsurface in the Hanford Tank Farms contained the same percentage of water as the calibration

standards, then the calibration and the log measurements would both involve water-bearing media. The radionuclide concentrations calculated with the calibration function would be in terms of decay activity per unit dry mass, and would be accurate.

However, most logging in the Tank Farms interrogates *unsaturated* media. Because there is no way to remove the water from the pore spaces in the calibration standards, it is not possible to match the calibration condition to the normal field condition. All that can be done is to estimate the largest potential error that could result from the water content mismatch between calibration standard and logged medium.

An error estimate can be gained from consideration of the SBM standard. The partial density due to water is estimated to be 0.25 grams per cubic centimeter, and the dry bulk density is reported as 1.87 grams per cubic centimeter Leino et al. (1994). Thus, the in situ bulk density is about 2.12 grams per cubic centimeter, but if the water could be entirely evacuated from the pore spaces in SBM, the bulk density would drop to 1.87 grams per cubic centimeter. Removal of the water would not change the number of gamma-ray emitters per unit volume, and Wilson and Stromswold (1981) showed that for a fixed number of gamma-ray emitters per unit volume, the gamma-ray flux in a medium is inversely proportional to the bulk density of the medium. This implies that removal of water from SBM would lead to a gamma-ray flux increase by a factor of about 1.13 (i.e.,  $(2.12)/(1.87)$ ).

The value of the calibration function (Equation 1-1) at a particular gamma-ray energy is proportional to the gamma-ray source intensity, in gammas per second per gram of sample material, and inversely proportional to the intensity of the spectral peak. Calibration functions are currently established using source intensities calculated from the dry mass concentrations and spectral peak intensities derived from spectra taken from water-bearing calibration media. For the SBM standard, the measured peak intensities could be converted to the values that would be recorded with water absent from the standard by multiplying each intensity by 1.13, if the water content is actually 0.25 grams per cubic centimeter. However, the water contents of SBM and the other standards are not well founded, so these conversions have not been done.

Because the unconverted peak intensities are too low by an approximate factor of 1.13, and because these peak intensities occur in the denominator of the calibration function, it follows that the calibration function, and hence, the radionuclide concentrations calculated with the calibration function, may be too high by approximately 14 percent.

The estimated 14 percent offset is a maximum error that applies to log measurements of completely dry formations. If the logged formation is not dry, then the gamma-ray signal is reduced, relative to a dry formation, by attenuation of gamma rays by water in the formation pore spaces. In that case, the calculated radionuclide concentration will be smaller, (i.e., closer to the true concentration). The calculated concentration will coincide with the true concentration if the water content of the logged formation is equal to the water content of the calibration standard.

## 2.2 Data Acquisition

Every spectrum for calibration and linearity demonstrations was acquired with the sonde held stationary and centered in the dry, open (uncased) 4.5-inch-diameter test hole of the particular calibration standard. For each test configuration, ten spectra were collected over an acquisition time of 1,000 seconds per spectrum. The collection of ten spectra for 1,000 seconds each, rather than fewer spectra for longer counting times, increased the likelihood that any equipment malfunctions that occurred during the data acquisitions would not go undetected. The 1,000-second counting time per spectrum was short enough to control spectral line broadening caused by gain shift during the acquisition of a spectrum.

Spectra for the water-filled-borehole correction study were collected by the same methods, except the test hole was filled with water during data acquisition.

## 2.3 Data Analysis

In December 1998 MACTEC-ERS' technical staff members decided that the version of the spectrum analysis software then in use, version 5.30, release 6 of *PCMCA/WIN* (Aptec Engineering Limited, North Tonawanda, New York), should be replaced by version 6.3.1, release 13. The main reason was Aptec Engineering's decision to terminate support for version 5.30. The replacement of version 5.30 with version 6.3.1 was completed on all project computers by January 31, 1999.

Because the sixth recalibration would be the first use of *PCMCA/WIN* version 6.3.1 to analyze calibration data, a cursory investigation was undertaken to show that results calculated with the new program contain no systematic offsets with respect to results calculated with the old program. The raw data for the investigation consisted of the sixth recalibration spectra collected by logging the SBK and SBM standards with Gamma 2A. The SBK ( $^{40}\text{K}$  enhanced) standard provided a low total count gamma-ray spectrum with a few intense gamma-ray fluxes, and the SBM ( $^{40}\text{K}$ ,  $^{238}\text{U}$ , and  $^{232}\text{Th}$  enhanced) standard provided a higher total count gamma-ray spectrum with many intense gamma-ray fluxes.

The calibration spectra from SBK and SBM were analyzed with both versions of *PCMCA/WIN* using the *peaksearch* and *multifit* algorithms. All of the user-specified software settings were identical to those customarily used for analysis of field data. The analysis method used for field data was applied, with two exceptions. Whereas field spectra are normally energy-calibrated by "importing" an energy calibration from a field verification spectrum, the calibration spectra were individually calibrated for energy using spectral peaks associated with some of the following gamma rays: 295.2 keV ( $^{214}\text{Pb}$ , uranium series), 352.0 keV ( $^{214}\text{Pb}$ , uranium series), 609.3 keV ( $^{214}\text{Bi}$ , uranium series), 1460.8 keV ( $^{40}\text{K}$ ), 1120.3 keV ( $^{214}\text{Bi}$ , uranium series), 1764.5 keV ( $^{214}\text{Bi}$ , uranium series), 2204.1 keV ( $^{214}\text{Bi}$ , uranium series), and 2614.5 keV ( $^{208}\text{Tl}$ , thorium series). Whereas field spectra are usually resolution-calibrated by importing a resolution calibration from a field verification spectrum, the calibration spectra were individually calibrated for resolution using the *resolution calibration* algorithm.

Average values for the FWHM and peak intensities were calculated for the ten spectra from each standard. Some averages for representative peaks are displayed in Tables 2-3 and 2-4. In all cases, a parameter value calculated with software version 6.3.1 agrees, within the experimental uncertainties (one standard deviation), with its counterpart calculated with version 5.30. In addition, the relative differences (in the fifth columns of both tables) appear to be random and not systematic. These observations suggest that differences between the calibration constants for the sixth recalibration and the constants for the earlier recalibrations (discussed in Section 4.0) can be attributed to shifts in system performances, and not to the software change.

*Table 2-3. PCMCA/WIN Comparison of SBK Data*

<b>Gamma-Ray Energy (keV)</b>	<b>Spectral Peak Parameter</b>	<b>Calculated with Version 5.30, Release 6 (uncertainty is one standard deviation)</b>	<b>Calculated with Version 6.3.1, release 13 (uncertainty is one standard deviation)</b>	<b>% Difference Between 5.30 and 6.3.1</b>
295.2	FWHM (keV)	$1.453 \pm 0.077$	$1.518 \pm 0.100$	-4.48
	intensity (c/s)	$0.667 \pm 0.054$	$0.664 \pm 0.061$	0.48
609.3	FWHM (keV)	$1.688 \pm 0.099$	$1.698 \pm 0.070$	-0.59
	intensity (c/s)	$1.217 \pm 0.083$	$1.211 \pm 0.092$	0.47
1238.1	FWHM (keV)	$2.074 \pm 0.062$	$2.103 \pm 0.058$	-1.39
	intensity (c/s)	$0.171 \pm 0.021$	$0.168 \pm 0.018$	1.83
1460.8	FWHM (keV)	$2.258 \pm 0.125$	$2.217 \pm 0.075$	1.82
	intensity (c/s)	$11.57 \pm 0.57$	$11.55 \pm 0.72$	0.22
1764.5	FWHM (keV)	$2.42 \pm 0.19$	$2.40 \pm 0.11$	0.81
	intensity (c/s)	$0.324 \pm 0.028$	$0.322 \pm 0.029$	0.74
2614.5	FWHM (keV)	$2.75 \pm 0.71$	$2.90 \pm 0.24$	-5.74
	intensity (c/s)	$0.056 \pm 0.011$	$0.057 \pm 0.012$	-1.90

Table 2-4. *PCMCA/WIN Comparison of SBM Data*

Gamma-Ray Energy (keV)	Spectral Peak Parameter	Calculated with Version 5.30, Release 6 (uncertainty is one standard deviation)	Calculated with Version 6.3.1, Release 13 (uncertainty is one standard deviation)	% Difference Between 5.30 and 6.3.1
185.9	FWHM (keV)	$1.610 \pm 0.024$	$1.627 \pm 0.018$	-1.06
	intensity (c/s)	$25.6 \pm 1.2$	$26.0 \pm 1.4$	-1.71
270.3	FWHM (keV)	$1.659 \pm 0.022$	$1.675 \pm 0.015$	-0.96
	intensity (c/s)	$6.54 \pm 0.32$	$6.69 \pm 0.48$	-2.17
352.0	FWHM (keV)	$1.705 \pm 0.017$	$1.717 \pm 0.014$	-0.70
	intensity (c/s)	$136.1 \pm 4.1$	$135.9 \pm 4.1$	0.13
609.3	FWHM (keV)	$1.852 \pm 0.012$	$1.854 \pm 0.011$	-0.11
	intensity (c/s)	$137.4 \pm 3.5$	$136.6 \pm 3.7$	0.56
911.1	FWHM (keV)	$2.024 \pm 0.014$	$2.018 \pm 0.012$	0.32
	intensity (c/s)	$21.90 \pm 0.44$	$21.89 \pm 0.47$	0.05
1120.3	FWHM (keV)	$2.138 \pm 0.015$	$2.129 \pm 0.017$	0.42
	intensity (c/s)	$39.27 \pm 0.98$	$39.28 \pm 1.04$	-0.02
1764.5	FWHM (keV)	$2.490 \pm 0.022$	$2.475 \pm 0.031$	0.60
	intensity (c/s)	$37.51 \pm 0.67$	$37.50 \pm 0.72$	0.03
2614.5	FWHM (keV)	$2.930 \pm 0.062$	$2.931 \pm 0.055$	-0.03
	intensity (c/s)	$21.75 \pm 0.25$	$21.60 \pm 0.38$	0.68

All of the calibration spectra were analyzed with *PCMCA/WIN* version 6.3.1, release 13. Spectral peaks were identified using the *peaksearch* algorithm, and the peak intensities were calculated with the *multifit* algorithm. The peak intensities calculated by the *multifit* algorithm were the (numerical) integrals of Gaussian functions that were fitted to the peaks using resolution calibration functions that were manually determined for each spectrum, as described in Section 5.0 of DOE (1998). All of the peak intensities were corrected for the logging system dead time by the method described in Section 3.0.

Because ten spectra were acquired for each calibration standard, there were generally ten peak intensities for each significant gamma ray associated with a calibration standard. Each set of ten intensities was examined for entries that differed significantly from the mean of the set. These “outliers” were removed from the data sets if the deletions were justified by the Chauvenet criterion (Friedlander et al. 1981). According to this criterion, rejection of a datum is justified if the difference between the datum and the mean has a probability of occurrence that is less than  $1/(2N)$ , where  $N$  is the number of elements in the set. The probability is calculated under the assumption that the data are normally distributed.

The weighted average for each set of dead-time-corrected intensities (with outliers removed) was calculated and used as the representative intensity. The weighted average was calculated using

$$\text{weighted average } P = \langle P \rangle = \frac{\sum_{i=1}^{10} P_i w_i}{\sum_{i=1}^{10} w_i}. \quad (2-1)$$

Each weight  $w_i$  in Equation (2-1) is the inverse square of the associated peak intensity uncertainty (95 percent confidence or 2s uncertainty):

$$w_i = \frac{1}{(2s_{P_i})^2}. \quad (2-2)$$

The 2s uncertainty in  $\langle P \rangle$  was calculated as follows:

$$2s_{\langle P \rangle} = \frac{1}{\sqrt{\sum_{i=1}^{10} w_i}}. \quad (2-3)$$

## 2.4 Calibration Functions and Recalibration Results

A calibration function  $I(E)$  was determined for each logging system by methods established for earlier calibrations and recalibrations. Dead-time-corrected weighted average peak intensities for representative gamma rays were used, along with the associated gamma-ray source intensities, to calculate values of  $I(E)$  for the energies of the representative gamma rays:

$$I(E) = \frac{\text{source intensity (in gammas per second per gram)}}{\text{weighted average peak intensity (in counts per second)}}. \quad (2-4)$$

The source intensities were calculated with a modified form of Equation (33) in DOE (1995b):

$$\text{source intensity} = \frac{(\text{gamma yield})(\text{concentration})}{27.027 \text{ picocuries per decay per second}}. \quad (2-5)$$

The gamma yields, in gammas per decay, were taken from Erdtmann and Soyka's (1979) compilation of gamma-ray data, and the potassium, radium, and thorium concentrations, in picocuries per gram, from Leino et al. (1994) were used. The source intensities, in units of gammas per second per gram of calibration standard material, are listed in Table 2-2 of DOE (1998b).



Tables 2-5 through 2-8 list the weighted average spectral peak intensities that were used to calculate the specific values for  $I(E)$ .

*Table 2-5. Weighted Average Spectral Peak Intensities for Gamma 1A*

<b>Gamma-Ray Energy (keV)</b>	<b>SBK Average Spectral Peak Intensity (c/s)</b>	<b>SBU Average Spectral Peak Intensity (c/s)</b>	<b>SBT Average Spectral Peak Intensity (c/s)</b>	<b>SBM Average Spectral Peak Intensity (c/s)</b>
129.1	no data <sup>2</sup>	no data	$2.23 \pm 0.37$	$4.02 \pm 0.82$
185.7, 186.0 <sup>1</sup>	$0.22 \pm 0.12$	$42.22 \pm 0.40$	$2.05 \pm 0.41$	$28.11 \pm 0.39$
238.6	no data	$4.44 \pm 0.46$	$94.3 \pm 1.8$	$3.20 \pm 0.50$
241.0, 241.9	no data	$29.18 \pm 0.49$	no data	$60.48 \pm 0.63$
270.3	no data	$4.85 \pm 0.39$	$6.78 \pm 0.14$	$7.53 \pm 0.30$
277.4	no data	$2.78 \pm 0.29$	$4.33 \pm 0.13$	$1.85 \pm 0.31$
295.2	$0.782 \pm 0.034$	$121.4 \pm 1.3$	$6.43 \pm 0.18$	$80.46 \pm 0.59$
300.1	no data	$2.3 \pm 2.6$	$6.26 \pm 0.18$	$5.01 \pm 0.36$
328	no data	no data	$5.87 \pm 0.16$	$3.48 \pm 0.31$
338.4	no data	no data	$21.82 \pm 0.21$	$14.10 \pm 0.33$
351.1, 352.0	$1.396 \pm 0.031$	$227.7 \pm 2.3$	$12.53 \pm 0.15$	$151.1 \pm 1.1$
462.1, 463.0	no data	no data	no data	no data
583.0, 583.1	no data	$2.11 \pm 0.28$	$48.08 \pm 0.25$	$30.96 \pm 0.27$
609.3	$1.443 \pm 0.034$	$231.5 \pm 2.8$	$12.735 \pm 0.089$	$152.7 \pm 1.2$
727.1	no data	no data	$11.038 \pm 0.086$	$7.11 \pm 0.13$
768.4	$0.134 \pm 0.047$	$24.49 \pm 0.46$	$0.75 \pm 0.14$	$7.39 \pm 0.18$
785.4	no data	$5.538 \pm 0.091$	$1.70 \pm 0.14$	$1.80 \pm 0.11$
794.8	no data	no data	$6.35 \pm 0.17$	$4.19 \pm 0.12$
860.5	no data	no data	$6.514 \pm 0.058$	$4.245 \pm 0.080$
911.1	no data	no data	$38.76 \pm 0.22$	$25.07 \pm 0.18$
934.1	no data	$14.27 \pm 0.12$	$0.756 \pm 0.047$	$9.45 \pm 0.11$
964.1, 964.6	no data	$1.622 \pm 0.089$	$7.19 \pm 0.11$	$5.552 \pm 0.090$
968.9	no data	no data	$23.38 \pm 0.17$	$15.32 \pm 0.12$
1120.3	$0.379 \pm 0.018$	$67.71 \pm 0.64$	$3.722 \pm 0.052$	$44.49 \pm 0.38$
1238.1	$0.186 \pm 0.020$	$26.03 \pm 0.22$	$1.373 \pm 0.037$	$17.06 \pm 0.14$
1377.7	$0.127 \pm 0.014$	$17.87 \pm 0.16$	$0.938 \pm 0.041$	$11.84 \pm 0.11$
1408	no data	$10.43 \pm 0.11$	$0.550 \pm 0.030$	$6.701 \pm 0.082$
1459.2, 1460.8	$13.85 \pm 0.12$	$2.720 \pm 0.059$	$3.47 \pm 0.10$	$11.04 \pm 0.11$
1509.2	$0.057 \pm 0.007$	$9.172 \pm 0.088$	$0.468 \pm 0.031$	$5.935 \pm 0.087$
1587.9	no data	no data	$4.098 \pm 0.052$	$2.63 \pm 0.11$
1620.6	no data	no data	$1.962 \pm 0.037$	$1.230 \pm 0.059$
1729.6	$0.073 \pm 0.006$	$12.43 \pm 0.11$	$0.654 \pm 0.025$	$8.129 \pm 0.076$
1764.5	$0.385 \pm 0.014$	$65.19 \pm 0.82$	$3.544 \pm 0.043$	$42.83 \pm 0.36$
1847.4	$0.041 \pm 0.005$	$8.46 \pm 0.09$	$0.427 \pm 0.026$	$5.609 \pm 0.065$
2204.1	$0.102 \pm 0.006$	$19.21 \pm 0.19$	$1.043 \pm 0.033$	$12.67 \pm 0.12$
2614.5	$0.069 \pm 0.005$	$0.425 \pm 0.020$	$38.74 \pm 0.22$	$25.42 \pm 0.24$

<sup>1</sup> A pair of numbers in the *Gamma-Ray Energy* column indicates that two gamma rays with the

indicated energies contributed to a single spectral peak.

<sup>2</sup> No data indicates that the spectral peak was too weak to analyze or that the peak intensity was incorrect because of interferences.

*Table 2-6. Weighted Average Spectral Peak Intensities for Gamma 1B*

<b>Gamma-Ray Energy (keV)</b>	<b>SBK Average Spectral Peak Intensity (c/s)</b>	<b>SBU Average Spectral Peak Intensity (c/s)</b>	<b>SBT Average Spectral Peak Intensity (c/s)</b>	<b>SBM Average Spectral Peak Intensity (c/s)</b>
129.1	no data	$3.2 \pm 1.2$	no data	no data
	no data	no data	no data	$25.72 \pm 0.82$
238.6	no data	$4.83 \pm 0.75$	$89.5 \pm 1.7$	$56.5 \pm 1.5$
241.0, 241.9	$0.287 \pm 0.075$	$45.51 \pm 0.72$	no data	$56.9 \pm 1.9$
270.3	no data	$4.49 \pm 0.40$	$6.65 \pm 0.18$	$6.98 \pm 0.35$
277.4	no data	$2.67 \pm 0.50$	$4.12 \pm 0.17$	$2.20 \pm 0.39$
295.2	$0.729 \pm 0.029$	$113.98 \pm 0.95$	$6.38 \pm 0.22$	$77.32 \pm 0.71$
300.1	no data	no data	$6.24 \pm 0.21$	$4.87 \pm 0.68$
328	no data	no data	$5.78 \pm 0.23$	$3.93 \pm 0.49$
338.4	no data	no data	$21.41 \pm 0.28$	$15.29 \pm 0.54$
351.1, 352.0	$1.406 \pm 0.037$	$215.4 \pm 2.2$	$12.20 \pm 0.21$	$149.9 \pm 1.0$
462.1, 463.0	no data	no data	no data	no data
583.0, 583.1	no data	$1.75 \pm 0.21$	$48.19 \pm 0.28$	$31.35 \pm 0.40$
609.3	$1.445 \pm 0.031$	$225.0 \pm 2.5$	$12.87 \pm 0.12$	$154.12 \pm 0.88$
727.1	no data	no data	$11.226 \pm 0.084$	$7.09 \pm 0.12$
768.4	$0.158 \pm 0.032$	$23.79 \pm 0.42$	$1.291 \pm 0.090$	$15.98 \pm 0.28$
785.4	no data	$5.366 \pm 0.079$	$1.80 \pm 0.10$	$4.54 \pm 0.17$
794.8	no data	no data	$6.45 \pm 0.10$	$3.98 \pm 0.17$
860.5	no data	no data	$6.640 \pm 0.066$	$4.163 \pm 0.094$
911.1	no data	$0.53 \pm 0.29$	$39.52 \pm 0.20$	$25.42 \pm 0.17$
934.1	no data	$14.06 \pm 0.12$	$0.789 \pm 0.041$	$9.46 \pm 0.12$
964.1, 964.6	no data	$1.515 \pm 0.074$	$7.577 \pm 0.094$	$5.731 \pm 0.093$
968.9	no data	no data	$23.94 \pm 0.16$	$15.52 \pm 0.13$
1120.3	$0.413 \pm 0.018$	$67.22 \pm 0.64$	$3.860 \pm 0.051$	$45.43 \pm 0.31$
1238.1	$0.194 \pm 0.020$	$25.71 \pm 0.24$	$1.463 \pm 0.037$	$17.37 \pm 0.13$
1377.7	$0.114 \pm 0.014$	$18.01 \pm 0.14$	$0.957 \pm 0.037$	$12.11 \pm 0.10$
1408	no data	$10.282 \pm 0.089$	$0.569 \pm 0.035$	$6.971 \pm 0.071$
1459.2, 1460.8	$13.94 \pm 0.12$	$2.604 \pm 0.063$	$3.49 \pm 0.10$	$11.37 \pm 0.10$
1509.2	$0.053 \pm 0.007$	$9.169 \pm 0.092$	$0.525 \pm 0.027$	$6.237 \pm 0.087$
1587.9	no data	no data	$4.276 \pm 0.052$	$2.83 \pm 0.10$
1620.6	no data	no data	$2.048 \pm 0.038$	$1.347 \pm 0.050$
1729.6	$0.069 \pm 0.005$	$12.49 \pm 0.12$	$0.666 \pm 0.027$	$8.384 \pm 0.077$
1764.5	$0.386 \pm 0.012$	$65.47 \pm 0.75$	$3.631 \pm 0.046$	$44.35 \pm 0.31$
1847.4	$0.040 \pm 0.004$	$8.667 \pm 0.086$	$0.465 \pm 0.023$	$5.750 \pm 0.064$
2204.1	$0.106 \pm 0.006$	$19.56 \pm 0.21$	$1.101 \pm 0.030$	$13.10 \pm 0.12$

2614.5	$0.063 \pm 0.005$	$0.444 \pm 0.019$	$40.59 \pm 0.23$	$26.63 \pm 0.21$
--------	-------------------	-------------------	------------------	------------------

*Table 2-7. Weighted Average Spectral Peak Intensities for Gamma 2A*

<b>Gamma-Ray Energy (keV)</b>	<b>SBK Average Spectral Peak Intensity (c/s)</b>	<b>SBU Average Spectral Peak Intensity (c/s)</b>	<b>SBT Average Spectral Peak Intensity (c/s)</b>	<b>SBM Average Spectral Peak Intensity (c/s)</b>
129.1	no data	$5.3 \pm 3.1$	$5.37 \pm 0.65$	$6.1 \pm 1.7$
185.7, 186.0	no data	$35.95 \pm 0.63$	$2.15 \pm 0.16$	$23.65 \pm 0.32$
238.6	no data	$2.5 \pm 1.1$	$77.9 \pm 2.7$	$51.3 \pm 1.4$
241.0, 241.9	$0.28 \pm 0.12$	$41.99 \pm 0.88$	no data	$51.0 \pm 1.2$
270.3	no data	$4.07 \pm 0.42$	$5.74 \pm 0.12$	$6.23 \pm 0.27$
277.4	no data	$2.53 \pm 0.54$	$3.71 \pm 0.11$	$2.26 \pm 0.31$
295.2	$0.608 \pm 0.026$	$104.19 \pm 0.82$	$5.51 \pm 0.17$	$67.56 \pm 0.95$
300.1	no data	no data	$5.54 \pm 0.16$	$4.13 \pm 0.70$
328	no data	no data	$4.89 \pm 0.18$	$3.18 \pm 0.34$
338.4	no data	no data	$18.33 \pm 0.22$	$12.26 \pm 0.32$
351.1, 352.0	$1.163 \pm 0.028$	$194.1 \pm 1.9$	$10.68 \pm 0.13$	$126.70 \pm 0.98$
462.1, 463.0	no data	no data	no data	no data
583.0, 583.1	no data	no data	$39.89 \pm 0.29$	$26.18 \pm 0.35$
609.3	$1.129 \pm 0.025$	$198.1 \pm 1.9$	$10.712 \pm 0.087$	$128.4 \pm 1.2$
727.1	no data	no data	$9.150 \pm 0.073$	$5.95 \pm 0.12$
768.4	$0.129 \pm 0.032$	$20.80 \pm 0.32$	$1.078 \pm 0.047$	$12.96 \pm 0.23$
785.4	no data	$4.766 \pm 0.078$	$1.563 \pm 0.050$	$3.74 \pm 0.11$
794.8	no data	no data	$5.302 \pm 0.070$	$3.46 \pm 0.10$
860.5	no data	no data	$5.473 \pm 0.056$	$3.480 \pm 0.074$
911.1	no data	no data	$31.91 \pm 0.18$	$20.65 \pm 0.18$
934.1	no data	$12.18 \pm 0.10$	$0.656 \pm 0.043$	$7.854 \pm 0.087$
964.1, 964.6	no data	$1.341 \pm 0.066$	$6.074 \pm 0.091$	$4.693 \pm 0.081$
968.9	no data	no data	$19.19 \pm 0.15$	$12.44 \pm 0.11$
1120.3	$0.320 \pm 0.015$	$57.40 \pm 0.52$	$3.078 \pm 0.039$	$37.01 \pm 0.30$
1238.1	$0.149 \pm 0.020$	$22.05 \pm 0.16$	$1.175 \pm 0.032$	$14.14 \pm 0.11$
1377.7	no data	$15.27 \pm 0.13$	$0.733 \pm 0.035$	$9.718 \pm 0.081$
1408	no data	$8.702 \pm 0.070$	$0.450 \pm 0.026$	$5.668 \pm 0.067$
1459.2, 1460.8	$10.92 \pm 0.17$	$2.221 \pm 0.055$	$2.74 \pm 0.10$	$9.12 \pm 0.11$
1509.2	$0.041 \pm 0.008$	$7.751 \pm 0.087$	$0.409 \pm 0.024$	$4.947 \pm 0.084$
1587.9	no data	no data	$3.314 \pm 0.056$	$2.210 \pm 0.095$
1620.6	no data	no data	$1.588 \pm 0.037$	$1.064 \pm 0.049$
1729.6	$0.053 \pm 0.005$	$10.30 \pm 0.10$	$0.512 \pm 0.022$	$6.663 \pm 0.065$
1764.5	$0.293 \pm 0.010$	$54.82 \pm 0.60$	$2.962 \pm 0.033$	$35.13 \pm 0.29$
1847.4	$0.033 \pm 0.004$	$7.112 \pm 0.080$	$0.358 \pm 0.022$	$4.541 \pm 0.053$
2204.1	$0.078 \pm 0.005$	$16.17 \pm 0.17$	$0.880 \pm 0.028$	$10.32 \pm 0.10$
2614.5	$0.052 \pm 0.004$	$0.350 \pm 0.016$	$31.49 \pm 0.30$	$20.91 \pm 0.21$

*Table 2-8. Weighted Average Spectral Peak Intensities for Gamma 2B*

<b>Gamma-Ray Energy (keV)</b>	<b>SBK Average Spectral Peak Intensity (c/s)</b>	<b>SBU Average Spectral Peak Intensity (c/s)</b>	<b>SBT Average Spectral Peak Intensity (c/s)</b>	<b>SBM Average Spectral Peak Intensity (c/s)</b>
129.1	no data	11.6 ± 11.2	3.30 ± 0.38	4.80 ± 0.83
185.7, 186.0	no data	40.71 ± 0.41	1.635 ± 0.004	27.35 ± 0.25
238.6	no data	4.12 ± 0.50	88.6 ± 2.7	60.4 ± 1.2
241.0, 241.9	0.291 ± 0.090	49.77 ± 0.57	no data	59.9 ± 1.7
270.3	no data	5.02 ± 0.49	6.57 ± 0.12	7.70 ± 0.37
277.4	no data	3.07 ± 0.75	4.19 ± 0.11	2.50 ± 0.39
295.2	0.741 ± 0.031	121.5 ± 1.5	6.62 ± 0.13	78.5 ± 1.2
300.1	no data	no data	6.43 ± 0.14	5.1 ± 1.4
328	no data	no data	5.48 ± 0.18	3.43 ± 0.22
338.4	no data	no data	21.24 ± 0.28	14.28 ± 0.26
351.1, 352.0	1.370 ± 0.037	230.3 ± 2.8	12.28 ± 0.15	150.1 ± 1.4
462.1, 463.0	no data	no data	no data	no data
583.0, 583.1	no data	no data	47.32 ± 0.36	31.56 ± 0.45
609.3	1.407 ± 0.024	239.3 ± 3.1	12.63 ± 0.12	155.2 ± 1.6
727.1	no data	no data	11.076 ± 0.079	7.43 ± 0.11
768.4	0.155 ± 0.021	25.30 ± 0.52	1.204 ± 0.050	15.81 ± 0.27
785.4	no data	5.74 ± 0.10	1.800 ± 0.051	4.64 ± 0.11
794.8	no data	no data	6.381 ± 0.070	4.13 ± 0.11
860.5	no data	no data	6.505 ± 0.060	4.353 ± 0.091
911.1	no data	no data	38.85 ± 0.26	26.05 ± 0.21
934.1	no data	14.97 ± 0.14	0.839 ± 0.041	9.75 ± 0.11
964.1, 964.6	no data	1.597 ± 0.076	7.27 ± 0.11	5.73 ± 0.10
968.9	no data	no data	23.50 ± 0.18	15.66 ± 0.14
1120.3	0.382 ± 0.018	70.96 ± 0.72	3.736 ± 0.042	46.27 ± 0.41
1238.1	0.168 ± 0.021	26.95 ± 0.25	1.438 ± 0.042	17.89 ± 0.14
1377.7	0.106 ± 0.012	18.99 ± 0.17	0.984 ± 0.036	12.47 ± 0.11
1408	no data	10.84 ± 0.10	0.562 ± 0.028	7.011 ± 0.069
1459.2, 1460.8	14.003 ± 0.091	2.810 ± 0.066	3.38 ± 0.14	11.55 ± 0.14
1509.2	0.050 ± 0.008	9.592 ± 0.080	0.518 ± 0.026	6.244 ± 0.083
1587.9	no data	no data	4.176 ± 0.063	2.88 ± 0.13
1620.6	no data	no data	2.018 ± 0.034	1.301 ± 0.058
1729.6	0.069 ± 0.006	13.19 ± 0.11	0.672 ± 0.027	8.563 ± 0.080
1764.5	0.393 ± 0.012	69.50 ± 0.78	3.570 ± 0.037	45.07 ± 0.52
1847.4	0.047 ± 0.005	9.05 ± 0.10	0.448 ± 0.028	5.859 ± 0.069
2204.1	0.113 ± 0.007	20.65 ± 0.22	1.080 ± 0.030	13.27 ± 0.12
2614.5	0.075 ± 0.005	0.466 ± 0.021	40.01 ± 0.25	27.02 ± 0.28

A functional representation for  $I(E)$ ,

$$I(E) = (C + D \ln(E))^2, \quad (2-6)$$

was determined for each logging system by analyzing the  $I(E)$  and  $E$  data with the *TableCurve* (version 1.11, Jandel Scientific Software, San Rafael, California) curve-fitting program. The factors  $C$  and  $D$  in Equation (2-6) have constant values for a particular logging system.

Figure 2-1 shows the  $I(E)$  data and the fitted curve determined with *TableCurve* for Gamma 1B. Similar results were derived for the three other logging systems.

The values of the constants  $C$  and  $D$  in the calibration function are displayed for the four logging systems in Table 1-2.

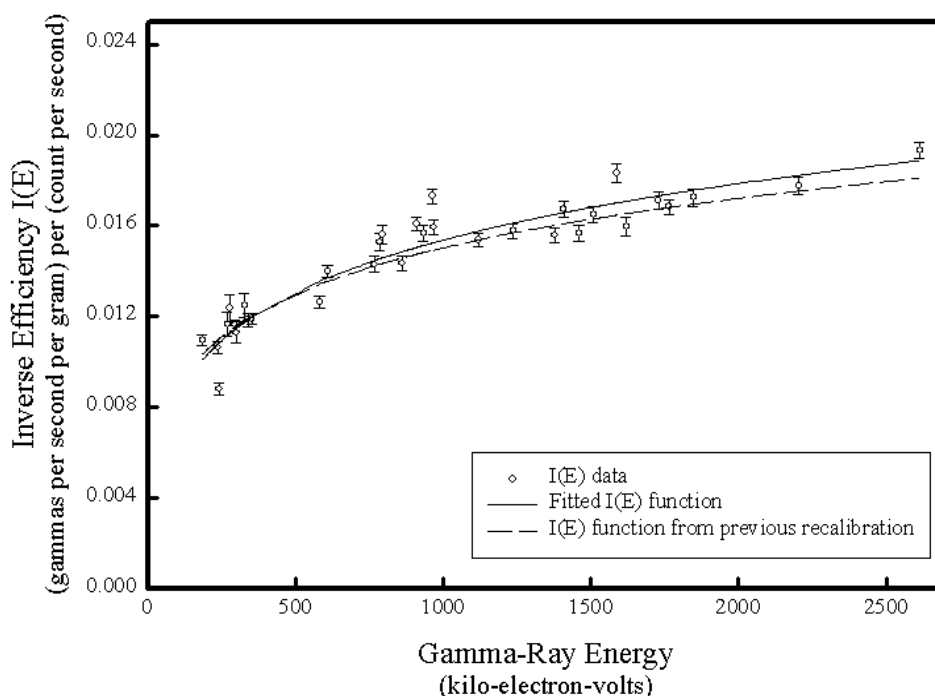


Figure 2-1. Data and Calibration Function for Gamma 1B. The calibration function from the previous recalibration is also shown for comparison.

These results are used as follows to calculate the concentration of a gamma-ray source. Analysis of a spectrum with the spectrum analysis program yields the intensity  $P$  of a spectral peak (in counts per second) and the energy  $E$  of the associated gamma ray. The gamma-ray source is identified using  $E$ .  $P$  is corrected for dead time and any other effects, such as borehole casing. The value of  $I(E)$  at the

particular  $E$  is calculated using Equation (2-6) and the constants  $C$  and  $D$  appropriate for the logging system. By definition,  $I(E)$  is the ratio of the gamma-ray source intensity to the corresponding (corrected) spectral peak intensity,  $P_C$ , so the intensity of the gamma-ray source  $S$ , in gamma rays per second per gram ( $\gamma/s/g$ ), is the product of  $I(E)$  and  $P_C$ :

$$S = I(E)P_C. \quad (2-7)$$

The concentration  $K$  of the gamma-ray source is

$$K = \frac{27.027}{Y} S = \frac{27.027}{Y} I(E)P_C. \quad (2-8)$$

In Equation (2-8),  $Y$  is the gamma-ray yield in gamma rays per decay and the conversion  $27.027 \text{ pCi} = 1 \text{ decay per second}$  accounts for the factor 27.027.

### 3.0 Linearity Test Results

Tests of Gamma 1 and Gamma 2 that were conducted before the base calibration indicated that the intensities of spectral peaks were not linearly related to the corresponding gamma-ray source intensities. The non-linearity was recognized as a manifestation of the electronic dead time effect. At low system dead times, the peak intensities are approximately linear in relation to gamma-ray source intensity, but at high system dead times, the peak intensities are smaller than would be predicted by the low dead time trend.

If the logging systems were used to assay just one radionuclide, the dead time effect could be ignored. Acquisition of calibration data would consist of recording spectra for a number of gamma-ray source intensities covering an adequate intensity range. Analyses of these spectral data would lead to a calibration equation expressing the relationship between spectral peak intensity and gamma-ray source intensity, and the relationship would be non-linear because of the dead time effect.

A dead time correction is needed because the logging systems are used to assay multiple radionuclides. The dead time rises or falls as the gamma-ray flux at the detector increases or decreases; consequently, the uncorrected intensity of the spectral peak for gamma rays from a source of constant intensity will go up or down if the flux at the detector due to a different source increases or decreases. The dead time correction counteracts this effect and restores the proportionality between the peak intensity and the intensity of the associated gamma-ray source.

A study of the system dead time effect is documented in the base calibration report (DOE 1995b). The study indicated that the dead time effect on the intensity of a spectral peak could be compensated (or corrected) by multiplying the peak intensity by a dead time correction:

$$\text{dead time correction} = \frac{1}{F \% G T_D \ln(T_D) \% H (T_D)^3} \quad (3-1)$$

$T_D$  is the percent dead time and  $F$ ,  $G$ , and  $H$  are dimensionless factors that have constant values for a particular logging system. The values of  $F$ ,  $G$ , and  $H$  determined by the analysis of base calibration data are displayed in Table 3-1.

Table 3-1. Factors for the Dead Time Correction

Logging Unit	$F$	$G$	$H$
Gamma 1A Gamma 1B	$1.0080 \pm 0.0054$	$(-4.71 \pm 0.47) \times 10^{-4}$	$(-5.73 \pm 0.21) \times 10^{-7}$
Gamma 2A Gamma 2B	$1.0322 \pm 0.0022$	$(-1.213 \pm 0.028) \times 10^{-3}$	$(-1.89 \pm 0.20) \times 10^{-7}$

The dead time correction study (DOE 1995b) indicated that the dead time corrections are independent of the gamma-ray energy.

The dead time corrections for Gamma 1A and Gamma 2A have not been directly reconfirmed since the base calibrations, and the dead time corrections for Gamma 1B and Gamma 2B have not been directly measured. However, the dead time corrections for all four systems have been indirectly validated at each recalibration using the fact that the dead time corrections establish linearity between corrected spectral peak intensities and gamma-ray source intensities. Thus, the validity of a dead time correction is confirmed if the relationship between corrected peak intensities and gamma-ray source concentrations is linear. These linearity demonstrations are part of each logging system recalibration.

For the sixth recalibration linearity demonstrations, spectra were acquired by logging all of the calibration standards listed in Table 2-1. The spectral peak intensities for several “radium” gamma rays were corrected for dead time, then plotted in relation to  $^{226}\text{Ra}$  concentration.  $^{226}\text{Ra}$  concentrations ranged from 1.16 picocuries per gram to 902 picocuries per gram, and the system dead times ranged from less than one percent to slightly higher than 70 percent.

All of the data conformed to the expected linear relationships. Some examples are presented in peak-intensity-versus-source-concentration plots in Figures 3-1, 3-2, 3-3, and 3-4.

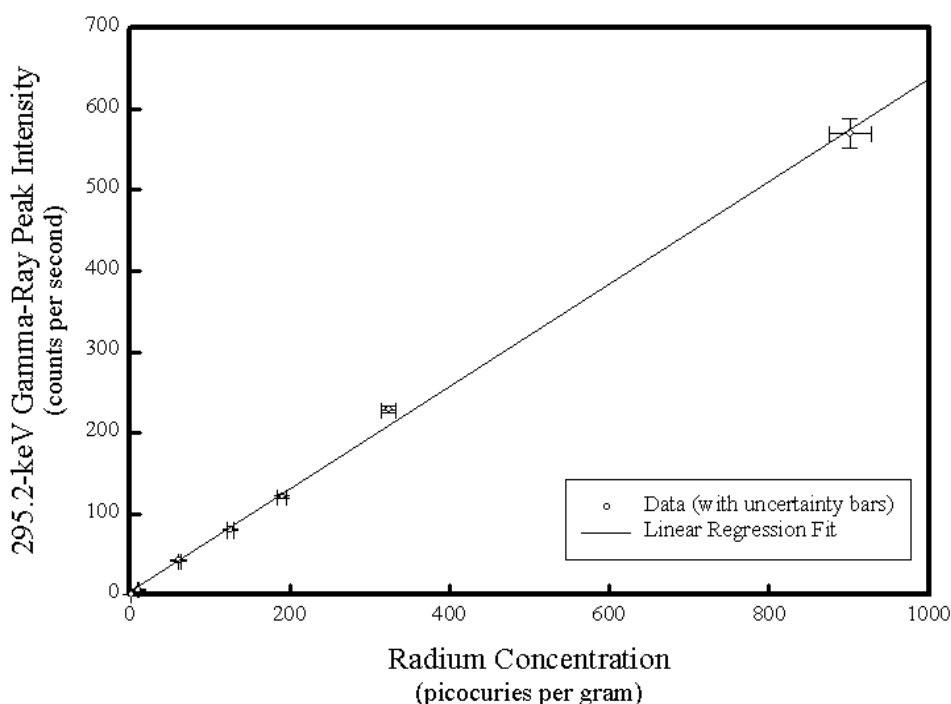


*Figure 3-1. Linearity Demonstration for Gamma 1A, 295.2-keV Gamma-Ray Data*



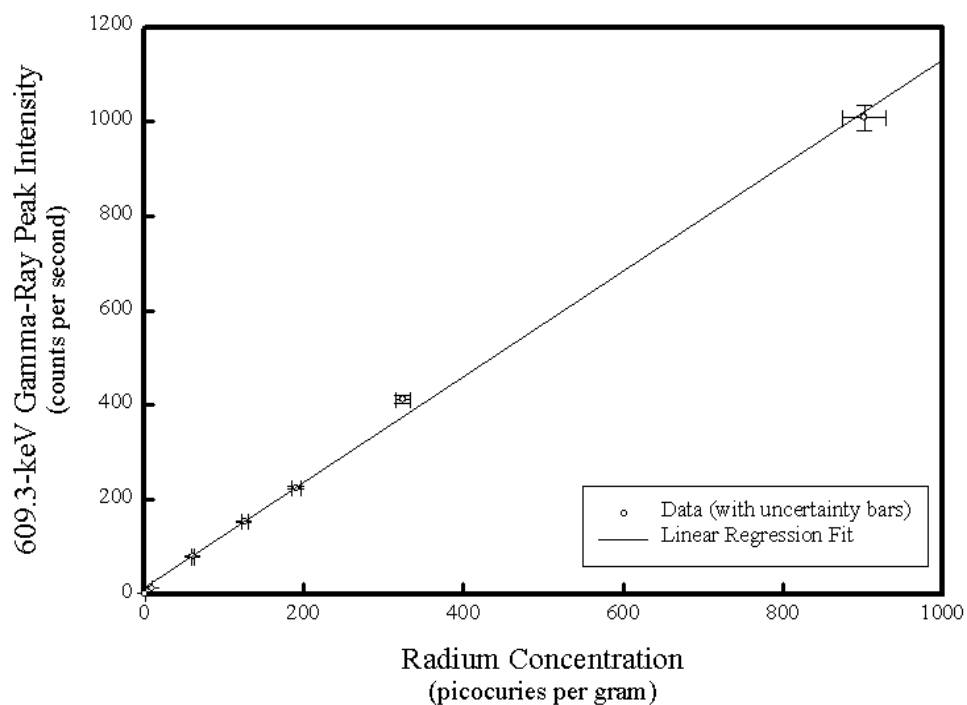


Figure 3-2. Linearity Demonstration for Gamma 1B, 609.3-keV Gamma-Ray Data

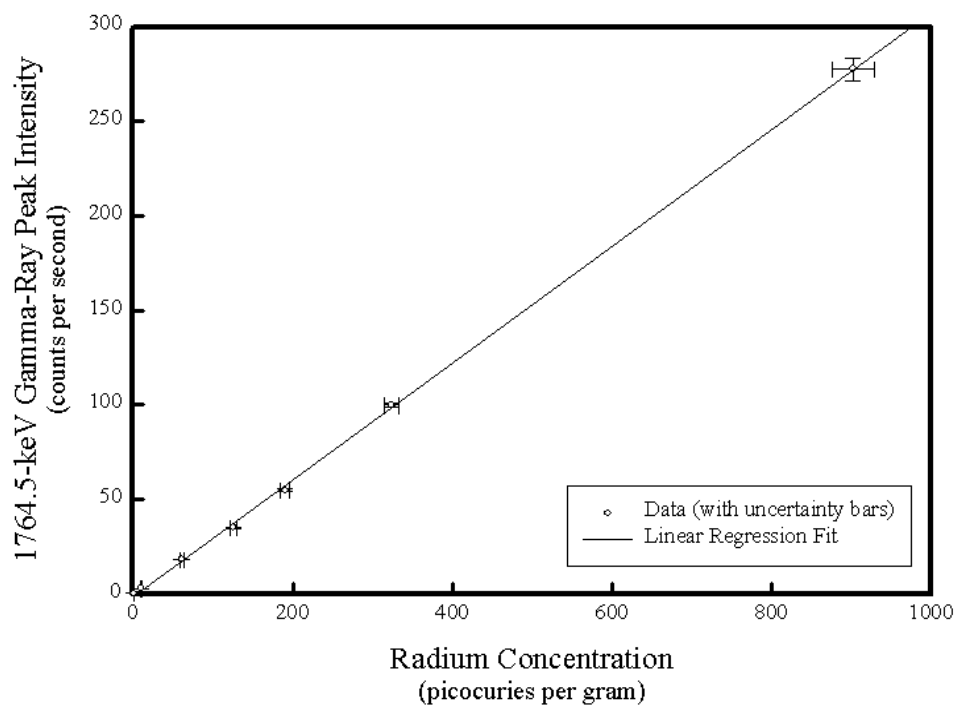
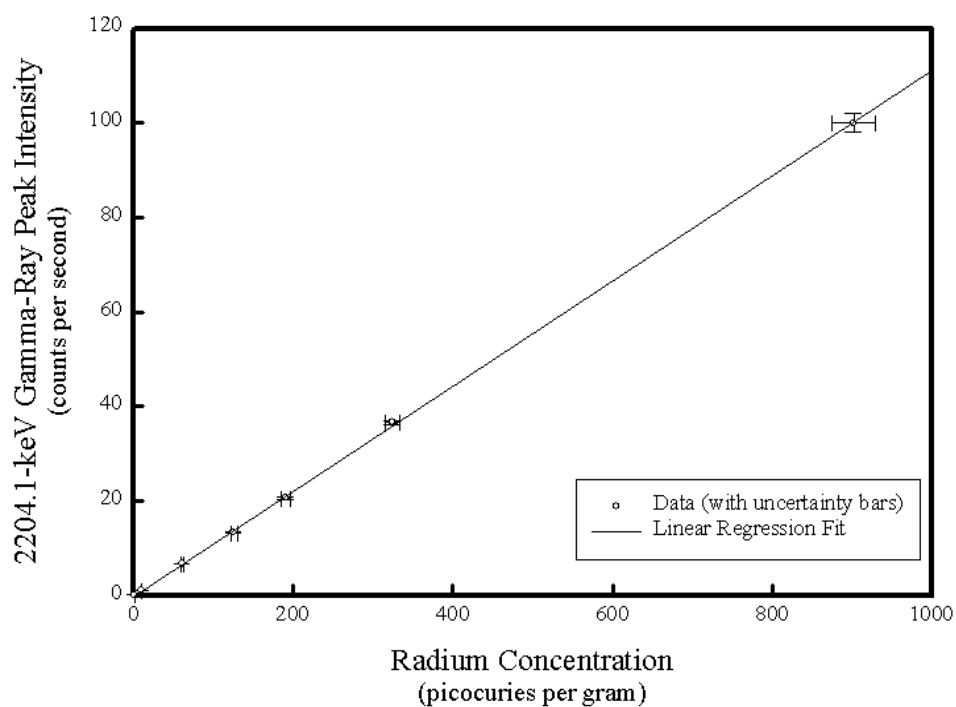


Figure 3-3. Linearity Demonstration for Gamma 2A, 1764.5-keV Gamma-Ray Data



*Figure 3-4. Linearity Demonstration for Gamma 2B, 2204.1-keV Gamma-Ray Data*

## 4.0 Comparison of Sixth Recalibration with Previous Recalibrations

Tables 4-1 and 4-2 display the calibration and recalibration constants for the four systems for all of the calibrations.

*Table 4-1. Calibration and Recalibration Constants for Gamma 1A and Gamma 1B*

	Gamma 1A		Gamma 1B	
Calibration	<i>C</i>	<i>D</i>	<i>C</i>	<i>D</i>
Base	$0.0195 \pm 0.0060$	$0.01511 \pm 0.00087$		
First Recalibration	$0.0182 \pm 0.0075$	$0.0149 \pm 0.0011$		
Second Recalibration	$0.0218 \pm 0.0073$	$0.0145 \pm 0.0011$		
Third Recalibration	$0.0149 \pm 0.0073$	$0.0153 \pm 0.0011$		
Fourth Recalibration	not calibrated	not calibrated	$0.0308 \pm 0.0066$	$0.0131 \pm 0.0010$
Fifth Recalibration	$0.0178 \pm 0.00032$	$0.01515 \pm 0.00048$	$0.0369 \pm 0.0029$	$0.01241 \pm 0.00043$
Sixth Recalibration	$0.0195 \pm 0.0036$	$0.01524 \pm 0.00054$	$0.0277 \pm 0.0041$	$0.01394 \pm 0.00061$

Note: No results prior to the fourth calibration are displayed for Gamma 1B because the backup sonde that is a component of Gamma 1B was acquired after the third recalibration.

*Table 4-2. Calibration and Recalibration Constants for Gamma 2A and Gamma 2B*

	Gamma 2A		Gamma 2B	
Calibration	<i>C</i>	<i>D</i>	<i>C</i>	<i>D</i>
Base	$0.0039 \pm 0.0058$	$0.01820 \pm 0.00083$		
First Recalibration	$0.00916 \pm 0.0087$	$0.0174 \pm 0.0013$		
Second Recalibration	$0.0101 \pm 0.0088$	$0.0174 \pm 0.0013$		
Third Recalibration	$0.0131 \pm 0.0085$	$0.0172 \pm 0.0012$		
Fourth Recalibration	$0.0181 \pm 0.0035$	$0.01641 \pm 0.00053$	$0.0310 \pm 0.0035$	$0.01305 \pm 0.00053$
Fifth Recalibration	$0.0165 \pm 0.0036$	$0.01665 \pm 0.00055$	$0.0341 \pm 0.0033$	$0.01271 \pm 0.00050$
Sixth Recalibration	$0.0093 \pm 0.0053$	$0.01846 \pm 0.00080$	$0.0242 \pm 0.0057$	$0.01433 \pm 0.00086$

Note: No results prior to the fourth calibration are displayed for Gamma 2B because the backup sonde that is a component of Gamma 1B was acquired after the third recalibration.

Because the variations in the calibration constants do not make the changes in system responses over time obvious, some hypothetical examples are presented as concrete illustrations of temporal changes in logging system performances.

The examples are based on three hypothetical source concentrations, 15 picocuries per gram of  $^{40}\text{K}$ , 20 picocuries per gram of  $^{137}\text{Cs}$ , and 20 picocuries per gram of  $^{60}\text{Co}$ , and spectral peaks associated with the 1460.8 keV, 661.6 keV, and 1173.2 keV gamma rays.

For each concentration, the count rate in the spectral peak was calculated using the assumption that the spectrum was recorded over a 100-second counting time by Gamma 1A, and using the Gamma 1A calibration constants from the base calibration.

The corresponding source intensities, in gammas per second per gram, were calculated with a modified form of Equation (2-8):

$$\text{source intensity} = \frac{(\text{gamma yield})(\text{concentration})}{27.027 \text{ picocuries per decay per second}}. \quad (4-1)$$

If the yield is in gammas per decay and the concentration is in picocuries per gram, then the source intensity will have units of gammas per second per gram.

Published yields for the three gamma rays (1460.8 keV, 661.6 keV, and 1173.2 keV) were used, along with the three hypothetical concentrations, to calculate source intensities for each of the three gamma rays. Each source intensity was then divided by the corresponding value of  $I(E)$ , calculated from

$$I(E) = (C \% D \ln(E))^2. \quad (4-2)$$

As stated earlier, the values of  $C$  and  $D$  ( $C = 0.0195 \pm 0.0060$ ,  $D = 0.01511 \pm 0.00087$ ) from the base calibration of Gamma 1A were used to calculate  $I(E)$ . Each ratio of source intensity to  $I(E)$  was a hypothetical spectral peak intensity. The results are summarized in Table 4-3.

*Table 4-3. Details of Three Hypothetical Gamma-Ray Sources*

Gamma-Ray Source	Gamma-Ray Energy (keV)	Source Concentration (pCi/g)	Source Intensity (γ/s/g)	$I(E)$ (γ/s/g) per (c/s)	Spectral Peak Intensity (c/s)
$^{40}\text{K}$	1460.8	15	0.0594	$0.0168 \pm 0.0023$	$3.535 \pm 0.376$
$^{137}\text{Cs}$	661.6	20	0.626	$0.0138 \pm 0.0019$	$45.24 \pm 1.35$
$^{60}\text{Co}$	1173.2	20	0.740	$0.0159 \pm 0.0022$	$46.40 \pm 1.36$

$^{40}\text{K}$ ,  $^{137}\text{Cs}$ , and  $^{60}\text{Co}$  concentrations were calculated using the hypothetical spectral peak intensities and the calibration constants  $C$  and  $D$  from the various calibrations. The results, tabulated in Table 4-4, are measures of the logging system efficiency changes over time.

*Table 4-4. Hypothetical Concentrations Illustrating Performances of Logging Systems over Time*

Logging System	Calibration	K Concentration (picocuries per gram)	Cs Concentration (picocuries per gram)	Co Concentration (picocuries per gram)
Gamma 1A	base	$15.0 \pm 2.6$	$20.0 \pm 2.9$	$20.0 \pm 2.8$
	recal 1	$14.4 \pm 2.9$	$19.1 \pm 3.5$	$19.1 \pm 3.4$
	recal 2	$14.5 \pm 2.9$	$19.4 \pm 3.5$	$19.4 \pm 3.4$
	recal 3	$14.3 \pm 2.9$	$18.9 \pm 3.4$	$19.0 \pm 3.3$
	recal 4	no cal	no cal	no cal
	recal 5	$14.7 \pm 1.8$	$19.5 \pm 1.2$	$19.6 \pm 1.2$
	recal 6	$15.2 \pm 2.0$	$20.3 \pm 1.8$	$20.3 \pm 1.8$
Gamma 1B	recal 4	$14.2 \pm 2.7$	$19.4 \pm 3.2$	$19.1 \pm 3.0$
	recal 5	$14.5 \pm 1.8$	$20.0 \pm 1.5$	$19.5 \pm 1.4$
	recal 6	$14.9 \pm 2.1$	$20.2 \pm 2.0$	$20.0 \pm 2.0$
Gamma 2A	base	$16.6 \pm 2.7$	$21.5 \pm 2.9$	$22.0 \pm 2.8$
	recal 1	$16.5 \pm 3.6$	$21.6 \pm 4.3$	$21.9 \pm 4.2$
	recal 2	$16.7 \pm 3.6$	$21.9 \pm 4.4$	$22.2 \pm 4.3$
	recal 3	$17.1 \pm 3.5$	$22.5 \pm 4.2$	$22.7 \pm 4.1$
	recal 4	$16.9 \pm 2.2$	$22.5 \pm 1.9$	$22.5 \pm 1.8$
	recal 5	$17.0 \pm 2.2$	$22.5 \pm 1.9$	$22.6 \pm 1.9$
	recal 6	$18.5 \pm 2.8$	$24.1 \pm 2.9$	$24.5 \pm 2.8$
Gamma 2B	recal 4	$14.2 \pm 1.9$	$19.4 \pm 1.7$	$19.0 \pm 1.7$
	recal 5	$14.3 \pm 1.9$	$19.7 \pm 1.7$	$19.3 \pm 1.6$
	recal 6	$14.8 \pm 2.5$	$19.9 \pm 2.8$	$19.7 \pm 2.7$

The entries in Table 4-4 support a conclusion stated in all previous calibration reports: For any particular logging system, a given spectral peak intensity can be analyzed with the calibration constants from any calibration, and the calculated concentrations will agree, within experimental uncertainties, with the concentrations calculated using the constants from any other calibration of the same logging system. In other words, the values for the calibration constants *C* and *D* have fluctuated over time, but the effects of these fluctuations on calculated concentrations have been so small that the logging systems can be regarded to have been essentially stable.

The hypothetical Gamma 1A concentrations are consistently smaller than the hypothetical Gamma 2A concentrations. This conforms to the observation that the efficiency of Gamma 1A has always been higher than the Gamma 2A efficiency.

The entries in Table 4-4 also reveal that the efficiency of Gamma 2B is nearly identical to the efficiency of Gamma 1B, but is offset from the efficiency of Gamma 2A. This suggests that the efficiency is dominated by the design and electronic components of the sonde, and not by the electronics mounted in the logging vehicles, indicating that a change in logging unit designations might be justified. The redesignation would replace four units, Gamma 1A, Gamma 1B, Gamma 2A, and Gamma 2B, with three units, Gamma 1 (presently known as Gamma 1A), Gamma 2 (presently known as Gamma 2A), and Gamma 3 (the backup sonde mounted on either logging vehicle). This change would yield some

project cost savings in calibration (three units instead of four would require periodic recalibration) and data processing. In addition, the data analysis software could be simplified.

The proposed new logging unit designations will be recommended if trends consistent with those described above are observed in the 1999 (seventh) recalibration results.

## 5.0 New Field Verification Criteria

A set of borehole measurements recorded sequentially in depth and time without changing the data acquisition parameters is a logging run. A borehole survey normally requires several logging runs, and the logging procedures specify that at least one field verification spectrum will be recorded before each logging run begins, and at least one additional spectrum will be recorded upon completion of each run. These field verification spectra are acquired with the sonde outside of the borehole and with an Amersham *KUTH Field Verifier* (Amersham part number 188074) gamma-ray source mounted on the sonde in a prescribed position relative to the detector.

Field verifications are a component in the logging program quality controls and serve as frequent confirmations of logging system efficiency and energy resolution. A system passes the efficiency check if the intensities of selected spectral peaks in the field verification spectra lie within acceptance limits. Likewise, the energy resolution is satisfactory if the FWHM of the selected spectral peaks fall within the acceptance limits. The peak intensity and FWHM limits, or tolerances, are updated at each recalibration. In the past, the acceptance limits for a logging system were derived as follows. Multitudinous field verification spectra taken with the logging system were processed, and the FWHM and peak intensities of selected spectral peaks were determined. For each spectral peak energy, the FWHM were placed in a set and the peak intensities were placed in another set. Then, for each set, two numbers, a lower acceptance limit and an upper acceptance limit, were calculated. The lower acceptance limit was the highest number (to two decimal places) that was less than the mean of the data set, and displaced far enough from the mean to be identified as a data outlier by the Chauvenet criterion (Friedlander et al. 1981). The upper acceptance limit was the lowest number (to two decimal places) that was greater than the mean of the data set, and displaced far enough from the mean to be identified as a data outlier by the Chauvenet criterion.

In the past, field verifications were conducted by recording spectra, calculating the FWHM and intensities of three or four peaks in each spectrum, and comparing these FWHM and intensities to the acceptance limits. The logging system was considered to be operating properly if the FWHM and peak intensities regularly fell between the acceptance limits. If a FWHM or peak intensity occasionally occurred outside of an acceptance range, no action was taken, but if readings outside of the range were consistently observed, field measurements were suspended and the logging system was checked for component malfunctions.

Over the duration of the logging project, each logging system has acquired a large number of field verification spectra. As the field verification databases expanded, the suitability of the Chauvenet criterion for acceptance limit determination diminished because the acceptance ranges were growing too wide as the numbers of elements in the data sets increased. The reason is that an element in a set is classified by the criterion as an outlier if the probability that an observation occurs as far, or farther, from the mean as the element is less than  $1/(2N)$ , where  $N$  is the number of elements in the data set. If the elements in a data set are normally distributed, then the area under the distribution curve that is within the acceptance range is  $1 - 1/(2N)$ , or  $(2N-1)/(2N)$ , and the area outside of the acceptance range is  $1/(2N)$ . As  $N$  for a data set grew large, the area under the distribution curve that was outside

of the acceptance range became so small that few, if any, field verification measurements differed from the data set mean by amounts large enough to qualify as data outliers.

At the sixth recalibration, the determination of acceptance criteria with the Chauvenet criterion was replaced as follows. Means and standard deviations ( $s$ ) were calculated for sets of data from all of the existing field verification spectra, and new acceptance criteria were established in two levels: a *warning limit* is exceeded if a measurement deviates from the corresponding mean by  $2s$  to  $3s$ , and a *control limit* is exceeded if a measurement deviates from the mean by  $3s$  or more.

To implement these limits, a field verification spectrum is recorded and the FWHM and peak intensities are calculated for the spectral peaks associated with three gamma rays: 609.3 keV, 1460.8 keV, and 2614.5 keV. These FWHM and peak intensities are compared to the appropriate warning and control limits. The logging system passes or fails the acceptance test according to the outcomes listed in Tables 5-1 and 5-2.

*Table 5-1. Outcomes of Field Verification Measurements*

<b>Test Result</b>	<b>Outcome</b>
The FWHM and peak intensities for all three peaks lie within the warning limits.	The system passes the acceptance test.
One of the six FWHM and intensities exceeds the warning limits, but not the control limits.	Data from the next (followup) spectrum are examined. An outcome is determined from Table 5-2.
Two or more of the six FWHM and intensities exceed the warning limits.	The system fails the acceptance test.
One or more of the six FWHM and intensities exceeds the control limits.	The system fails the acceptance test.



*Table 5-2. Outcomes of Field Verification Measurements Involving Followup Spectra*

<b>Test Result, Followup Spectrum</b>	<b>Outcome</b>
The FWHM and peak intensities for all three peaks lie within the warning limits.	The system passes the acceptance test.
The FWHM or intensity that exceeded the warning limits, but not the control limits, in the earlier measurement now falls within the warning limits, but a different FWHM or intensity falls outside of the warning limits, but not the control limits.	Data from the next (third) spectrum are analyzed, and this table (5-2) is used to determine the outcome.
The FWHM or intensity that exceeded the warning limits, but not the control limits, in the earlier measurement exceeds the warning limits again, and lies on the same side of the data set mean as before.	The system fails the acceptance test.
The FWHM or intensity that exceeded the warning limits, but not the control limits, in the earlier measurement exceeds the warning limits again, but lies on the opposite side of the data set mean.	Data from the next (third) spectrum are analyzed. If the same FWHM or intensity falls outside of the warning limits again, the system fails the acceptance test.
Two or more of the six FWHM and intensities exceed the warning limits.	The system fails the acceptance test.
One or more of the six FWHM and intensities exceeds the control limits.	The system fails the acceptance test.

The project Technical Lead must be notified of any acceptance test failure as soon as possible so that the cause of the failure can be determined and corrected.

For Gamma 1A, field verification data collected prior to January 23, 1998 were analyzed and the warning and control limits listed in Table 1-3 were derived from statistical analysis of 687 spectra. These acceptance criteria are applicable until new acceptance criteria are established by the next recalibration.

For Gamma 1B, field verification criteria were established from statistical analysis of 273 field verification spectra collected prior to May 20, 1998. Warning and control limits for Gamma 1-B are shown in Table 1-4. These acceptance criteria are applicable until new acceptance criteria are established by the next recalibration.

For Gamma 2A, field verification criteria were established from statistical analysis of 968 field verification spectra collected prior to September 22, 1998. Warning and control limits for Gamma 2A

are shown in Table 1-5. These acceptance criteria are applicable until new acceptance criteria are established by the next recalibration.

For Gamma 2B, field verification criteria were established from statistical analysis of 386 field verification spectra collected prior to March 12, 1999. Warning and control limits for Gamma 2B are shown in Table 1-6. These acceptance criteria are applicable until new acceptance criteria are established by the next recalibration.

## 6.0 Corrections for the 4.5-inch Water-Filled Borehole

In the standard logging configuration, the sonde is centralized in an air-filled borehole. Logging system calibrations have been determined for this configuration, so if spectra are collected by logging a water-filled borehole, the spectral peak intensities have to be corrected to account for gamma-ray attenuation by the water. Corrections for water-filled boreholes were determined for Gamma 1A and Gamma 2A from data that were acquired during the base calibration (DOE 1995b) and the first recalibration (DOE 1996a).

Base calibration data for the determination of corrections were acquired by logging the DOE-GJO KW Model (Leino et al. 1994). This standard has a mixture of potassium, uranium, and thorium sources and five test holes with diameters ranging from 3 inches to 12 inches. Sources with many gamma-ray energies and test holes with a range of diameters are the attributes needed to determine corrections that depend on the gamma-ray energy and the borehole diameter.

After the logging systems were dispatched to the Hanford Site, there was no convenient way to reconfirm the water corrections because all of the test holes in the calibration standards at Hanford have the same diameter (4.5 inches) and it is an expensive and time-consuming operation to transport the logging systems back to GJO (the distance between GJO and Hanford is about 1,000 miles). Therefore, water corrections have been applied to Hanford borehole data under the assumption that these corrections don't change over time.

The backup sonde was acquired in 1997, more than 2 years after completion of the base calibrations. Because the Hanford calibration models don't offer a range of borehole diameters, water correction measurements were not made with the backup sonde. Instead, it has been assumed that the water corrections for Gamma 1A are applicable to data acquired with Gamma 1B, and that the corrections for Gamma 2A can be applied to data acquired with Gamma 2B.

For the sixth recalibration, the Hanford standard SBM was logged with the air-filled test hole for the normal calibration measurements, and the standard was also logged with water in the test hole. With these data, the water corrections for the 4.5-inch-diameter borehole were determined for the four logging systems. These corrections were derived with the expectation that they would, upon comparison with the corrections from the base calibrations, support the two correction assumptions. In particular, if the new corrections for Gamma 1A and Gamma 2A agreed with the original Gamma 1A and Gamma 2A corrections, the contention that corrections are stable over time would be supported. Also, if the new corrections for Gamma 1B and Gamma 2B agreed, respectively, with the original corrections for Gamma 1A and Gamma 1B, it would add credibility to the thesis that the correction for either original sonde can be applied to data taken with the backup sonde.

Corrections for the 4.5-inch water-filled borehole were calculated using the same equation that was introduced in the base calibration report (DOE 1995b). That is, the correction for a particular gamma-ray energy  $E$  is

$$\text{correction} = K(E) \cdot \frac{\text{peak intensity from the air\&filled hole measurement}}{\text{peak intensity from the water\&filled hole measurement}} \quad (6-1)$$

The calculated corrections are displayed in Tables 6-1 and 6-2.

*Table 6-1. Corrections for Gamma 1A and Gamma 1B*

<b>Gamma-Ray Energy (keV)</b>	<b>Base Corrections for Gamma 1A</b>	<b>Sixth Recalibration Corrections for Gamma 1A</b>	<b>Sixth Recalibration Corrections for Gamma 1B</b>
185.9	1.699 ± 0.040	1.352 ± 0.025	1.324 ± 0.047
241.9	1.107 ± 0.078	1.330 ± 0.190	1.287 ± 0.047
270.3	no data	no data	1.286 ± 0.089
295.2	1.634 ± 0.033	1.283 ± 0.029	1.291 ± 0.019
338.4	no data	1.268 ± 0.036	no data
352.0	1.573 ± 0.015	1.268 ± 0.015	1.287 ± 0.016
583.1	1.541 ± 0.044	1.213 ± 0.019	1.219 ± 0.022
609.3	1.550 ± 0.013	1.215 ± 0.016	1.219 ± 0.014
727.1	no data	1.173 ± 0.041	1.203 ± 0.027
768.4	1.494 ± 0.047	1.197 ± 0.033	1.256 ± 0.037
785.4	no data	1.218 ± 0.047	1.181 ± 0.051
794.8	no data	no data	1.127 ± 0.054
860.5	no data	1.179 ± 0.034	1.138 ± 0.034
911.1	1.523 ± 0.038	1.176 ± 0.018	1.171 ± 0.013
934.1	1.567 ± 0.064	1.140 ± 0.020	1.160 ± 0.019
964.6	no data	1.194 ± 0.034	1.176 ± 0.029
968.9	1.388 ± 0.043	1.167 ± 0.015	1.174 ± 0.015
1120.3	1.473 ± 0.016	1.169 ± 0.013	1.155 ± 0.014
1238.1	1.489 ± 0.029	1.140 ± 0.013	1.146 ± 0.012
1377.7	1.356 ± 0.052	1.143 ± 0.014	1.150 ± 0.013
1408.0	1.414 ± 0.055	1.151 ± 0.020	1.135 ± 0.016
1460.8	1.426 ± 0.035	1.130 ± 0.017	1.130 ± 0.018
1509.2	1.445 ± 0.062	1.142 ± 0.033	1.148 ± 0.024
1587.9	no data	1.127 ± 0.088	1.153 ± 0.066
1729.6	1.391 ± 0.030	1.144 ± 0.017	1.134 ± 0.015
1764.5	1.355 ± 0.015	1.126 ± 0.013	1.126 ± 0.014
1847.4	1.469 ± 0.049	1.111 ± 0.029	1.108 ± 0.016
2204.1	1.324 ± 0.018	1.123 ± 0.014	1.107 ± 0.014
2614.5	1.279 ± 0.016	1.104 ± 0.015	1.103 ± 0.013

*Table 6-2. Corrections for Gamma 2A and Gamma 2B*

<b>Gamma-Ray Energy (keV)</b>	<b>Base Corrections for Gamma 2A</b>	<b>Sixth Recalibration Corrections for Gamma 2A</b>	<b>Sixth Recalibration Corrections for Gamma 2B</b>
185.9	$1.341 \pm 0.024$	$1.372 \pm 0.026$	$1.347 \pm 0.021$
241.0	$1.335 \pm 0.029$	no data	no data
241.9	$1.338 \pm 0.040$	$1.345 \pm 0.038$	no data
270.3	no data	$1.374 \pm 0.096$	$1.355 \pm 0.092$
295.2	$1.289 \pm 0.017$	$1.344 \pm 0.033$	$1.274 \pm 0.026$
328.0	no data	no data	$1.356 \pm 0.130$
338.4	no data	$1.312 \pm 0.047$	$1.292 \pm 0.034$
352.0	$1.276 \pm 0.017$	$1.296 \pm 0.015$	$1.258 \pm 0.018$
463.0	$1.239 \pm 0.058$	no data	no data
583.1	$1.226 \pm 0.019$	$1.253 \pm 0.023$	$1.213 \pm 0.024$
609.3	$1.209 \pm 0.021$	$1.234 \pm 0.018$	$1.210 \pm 0.018$
727.1	$1.153 \pm 0.029$	$1.203 \pm 0.031$	$1.204 \pm 0.028$
768.4	$1.182 \pm 0.034$	$1.228 \pm 0.032$	$1.203 \pm 0.032$
785.4	no data	$1.230 \pm 0.051$	$1.207 \pm 0.039$
794.8	no data	$1.237 \pm 0.052$	$1.193 \pm 0.044$
860.5	$1.205 \pm 0.046$	$1.161 \pm 0.038$	$1.175 \pm 0.035$
911.1	$1.176 \pm 0.018$	$1.177 \pm 0.014$	$1.178 \pm 0.014$
934.1	$1.183 \pm 0.026$	$1.178 \pm 0.018$	$1.181 \pm 0.019$
964.6	$1.160 \pm 0.030$	$1.169 \pm 0.028$	$1.182 \pm 0.029$
968.9	$1.180 \pm 0.015$	$1.172 \pm 0.015$	$1.166 \pm 0.014$
1120.3	$1.162 \pm 0.015$	$1.171 \pm 0.014$	$1.164 \pm 0.014$
1238.1	$1.158 \pm 0.015$	$1.173 \pm 0.012$	$1.163 \pm 0.012$
1377.7	$1.140 \pm 0.021$	$1.155 \pm 0.015$	$1.157 \pm 0.014$
1408.0	$1.121 \pm 0.023$	$1.155 \pm 0.020$	$1.143 \pm 0.018$
1460.8	$1.136 \pm 0.023$	$1.152 \pm 0.020$	$1.136 \pm 0.020$
1509.2	$1.142 \pm 0.029$	$1.178 \pm 0.029$	$1.152 \pm 0.025$
1587.9	no data	$1.160 \pm 0.075$	$1.153 \pm 0.072$
1620.6	no data	no data	$1.155 \pm 0.077$
1729.6	$1.112 \pm 0.021$	$1.148 \pm 0.017$	$1.151 \pm 0.015$
1764.5	$1.131 \pm 0.021$	$1.139 \pm 0.014$	$1.128 \pm 0.017$
1847.4	$1.138 \pm 0.028$	$1.135 \pm 0.020$	$1.135 \pm 0.021$
2204.1	$1.117 \pm 0.021$	$1.116 \pm 0.016$	$1.102 \pm 0.015$
2614.5	$1.120 \pm 0.033$	$1.113 \pm 0.017$	$1.105 \pm 0.017$

The entries in Table 6-2 for Gamma 2A and Gamma 2B conform to expectations, but the entries in Table 6-1 show that the Gamma 1A base corrections are obviously offset from the corresponding sixth recalibration corrections for Gamma 1A and the corrections for Gamma 1B. The Gamma 2A and

Gamma 2B results will be discussed first, then a reason for the Gamma 1A discrepancies will be presented, and corrective steps will be proposed.

Corrections for Gamma 2A and Gamma 2B are represented by symbols in the plots of Figure 6-1.

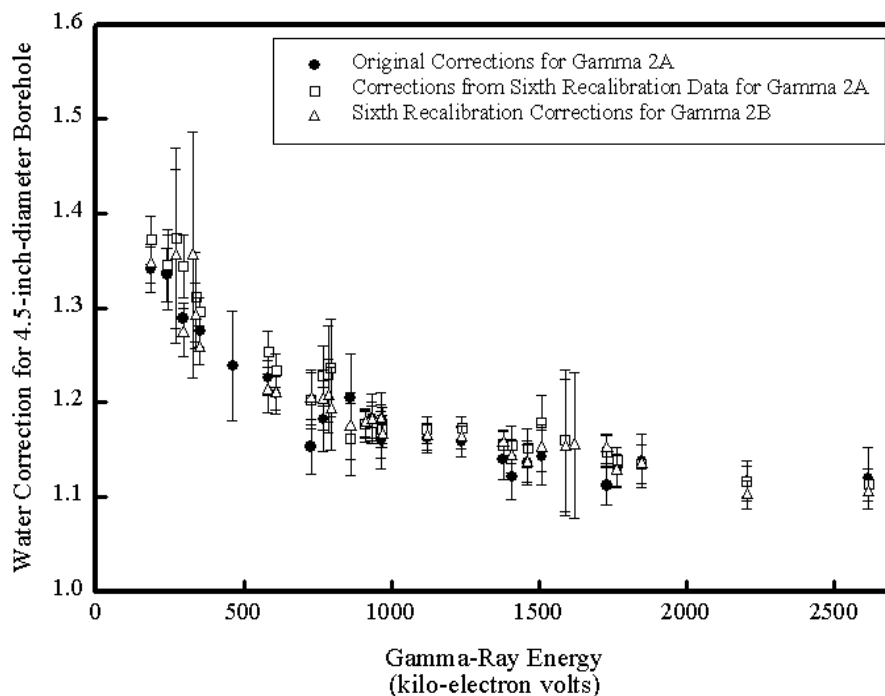


Figure 6-1. Calculated Water Corrections for Gamma 2A and Gamma 2B

Inspection of the entries in Table 6-2 and the data points in Figure 6-1 suggests that the three sets of corrections all coincide, within the experimental uncertainties.

Curve fitting analysis of each data set indicated that the corrections are well represented by

$$K(E) = \sqrt{A + \frac{B}{E}} \quad (6-2)$$

In Equation (6-2)  $A$  and  $B$  are constants and  $E$  is the gamma-ray energy in kilo-electron-volts. The values for  $A$  and  $B$  derived by curve fitting are displayed in Table 6-3.

Table 6-3. Constants A and B for the Water Corrections for Gamma 2A and Gamma 2B

Correction	$A \pm 2s A$ (dimensionless)	$B \pm 2s B$ (kilo-electron-volts)
Original (Base) Calibration Gamma 2A	$1.2230 \pm 0.0024$	$128.7 \pm 1.4$
Sixth Recalibration Gamma 2A	$1.2274 \pm 0.0022$	$150.7 \pm 1.6$
Sixth Recalibration Gamma 2B	$1.2326 \pm 0.0020$	$122.7 \pm 1.4$

The curves in Figure 6-2 depict the three corrections in relation to gamma-ray energy that are predicted by Equation 6-2 and the constants in Table 6-3.

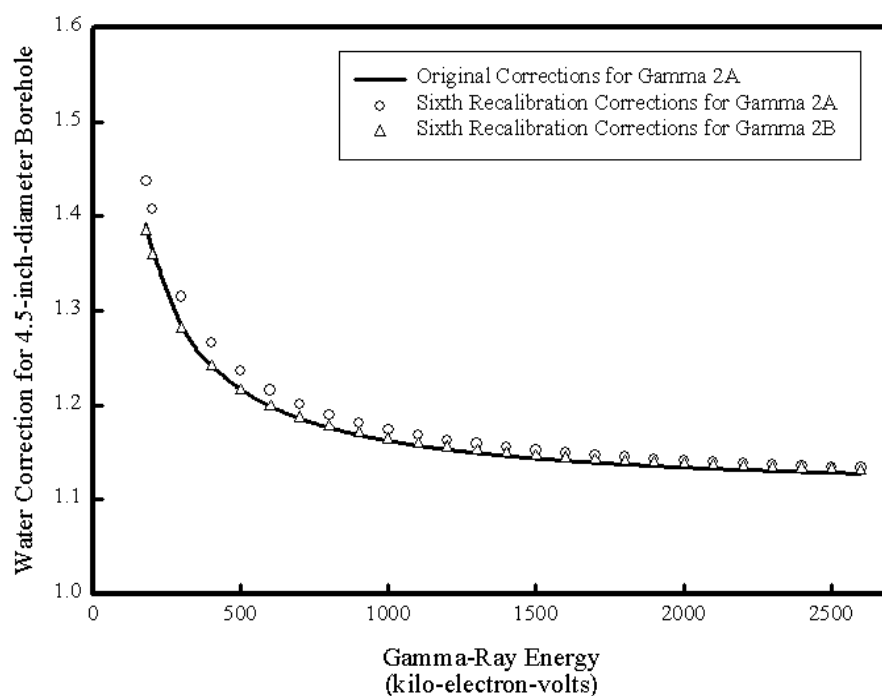


Figure 6-2. Original and Sixth Recalibration Water Corrections for Gamma 2, 4.5-inch Borehole

The corrections presented in Tables 6-1 and 6-2 and Figures 6-1 and 6-2 indicate that for Gamma 2A there are no significant differences between the 4.5-inch water corrections determined from the sixth recalibration and the corresponding corrections from the base calibration. Likewise, the corrections for Gamma 2B are identical, within experimental uncertainties, to the corrections for Gamma 2A. These comparisons strengthen the contentions that environmental corrections for the backup sonde are

identical to the corrections for the original sonde, and that the environmental corrections are stable over time and need not be reconfirmed at each recalibration.

One more observation shows that the three different 4.5-inch water corrections for Gamma 2A and Gamma 2B can be considered identical. The gamma-ray sources of primary interest to the Hanford logging are  $^{40}\text{K}$ ,  $^{226}\text{Ra}$  ( $^{238}\text{U}$ ),  $^{232}\text{Th}$ ,  $^{137}\text{Cs}$ , and  $^{60}\text{Co}$ . The entries in Table 6-4 show that the calculated water corrections for the principal gamma rays from these sources are essentially identical.

*Table 6-4. Gamma 2 Water Corrections for Gamma Rays of Primary Importance*

<b>Gamma-Ray Energy (keV)</b>	<b>Corrections for Gamma 2A Calculated with Equation 6-2 and the Baseline Constants</b>	<b>Corrections for Gamma 2A Calculated with Equation 6-2 and the Sixth Recalibration Constants</b>	<b>Corrections for Gamma 2B Calculated with Equation 6-2 and the Sixth Recalibration Constants</b>
609.3 ( $^{226}\text{Ra}$ )	1.198	1.214	1.197
661.6 ( $^{137}\text{Cs}$ )	1.191	1.206	1.191
1173.2 ( $^{60}\text{Co}$ )	1.154	1.164	1.156
1332.5 ( $^{60}\text{Co}$ )	1.149	1.158	1.151
1460.8 ( $^{60}\text{Co}$ )	1.145	1.154	1.147
1764.5 ( $^{226}\text{Ra}$ )	1.138	1.146	1.141
2614.5 ( $^{232}\text{Th}$ )	1.128	1.134	1.131

Unfortunately, the corrections for Gamma 1A and Gamma 1B did not conform to expectations as did the corrections for Gamma 2A and Gamma 2B. Figure 6-3 shows 4.5-inch water corrections plotted in relation to gamma-ray energy for Gamma 1A and Gamma 1B. One set of Gamma 1A corrections is from the base calibration, and the other Gamma 1A and the Gamma 1B corrections are from the sixth recalibration. The base corrections for Gamma 1A are consistently larger, by over 20 percent, than the corresponding corrections from the sixth recalibration for Gamma 1A and Gamma 1B, but the sixth recalibration corrections for Gamma 1A and Gamma 1B are nearly coincident. The most likely explanation of these observations is an electrical problem that plagued the base calibration measurements that were made with the Gamma 1A sonde immersed in water.

The possibility that the problem with the original corrections was caused by logging system components mounted in the Gamma 1 vehicle can be dismissed on the basis of the following observations. The system Gamma 1B consists of the backup sonde connected to the Gamma 1 logging vehicle, and Gamma 2B consists of the backup sonde connected to the Gamma 2 logging vehicle. Therefore, if the Gamma 1B and Gamma 2B correction data are identical (within experimental uncertainties), and are correct, then malfunctions of components in the logging vehicles can be ruled out. If the Gamma 1A original corrections are erroneous, the problem must be in the original sonde associated with the Gamma 1 logging system.



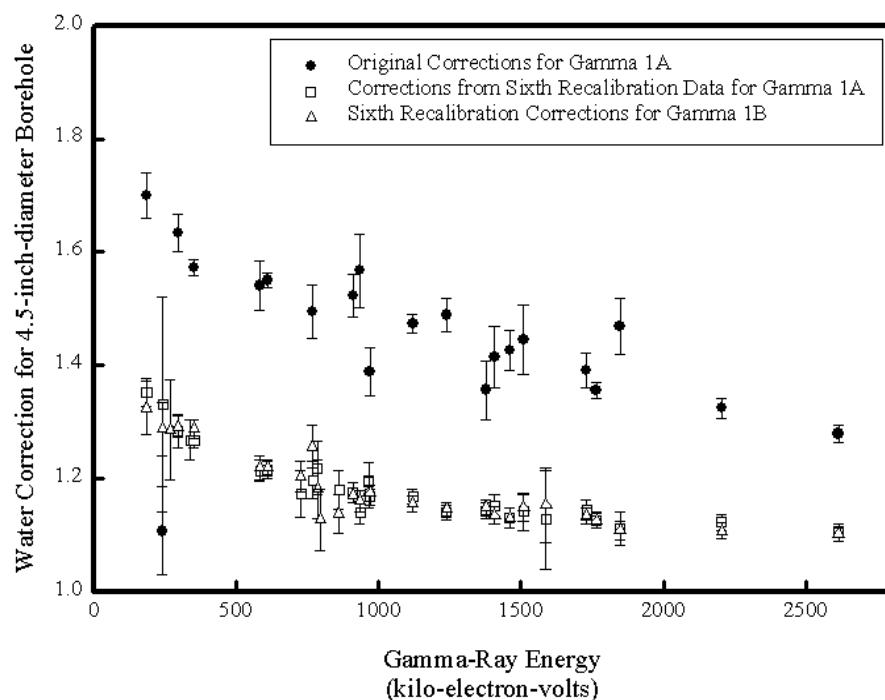


Figure 6-3. Three Sets of Water Corrections for Gamma 1

Figures 6-4 and 6-5 show typical calibration spectra that were recorded by logging the SBB calibration standard with Gamma 1B. The spectrum in Figure 6-4 was recorded without water in the test hole, and the spectrum in Figure 6-5 was recorded with the sonde immersed in water.

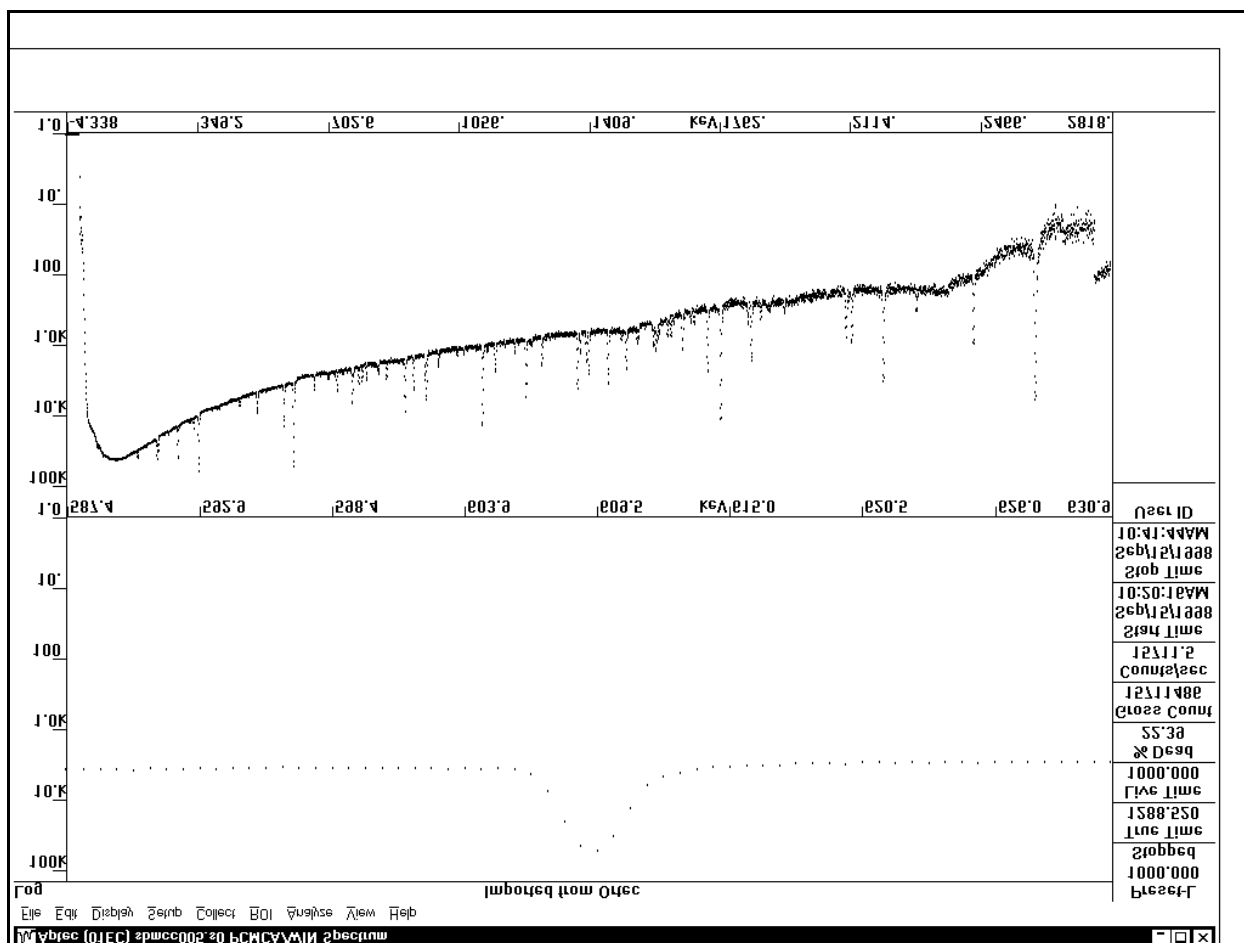
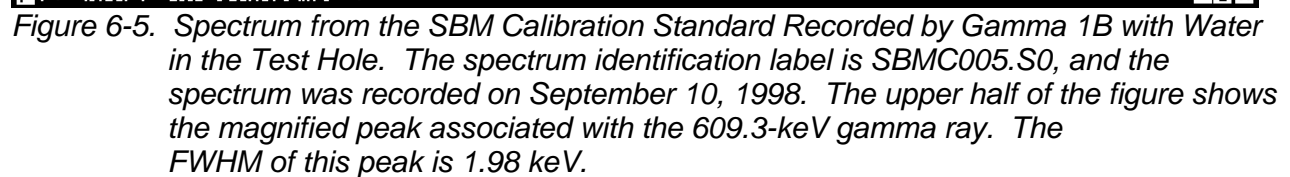


Figure 6-4. Spectrum from the SBM Calibration Standard Recorded by Gamma 1B Without Water in the Test Hole. The spectrum identification label is SBMCC005.S0, and the spectrum was recorded on September 15, 1998. The upper half of the figure shows the magnified peak associated with the 609.3-keV gamma ray. The FWHM of this peak is 2.02 keV.



A typical base calibration spectrum recorded with Gamma 1A with water in the test hole is shown in Figure 6-6.

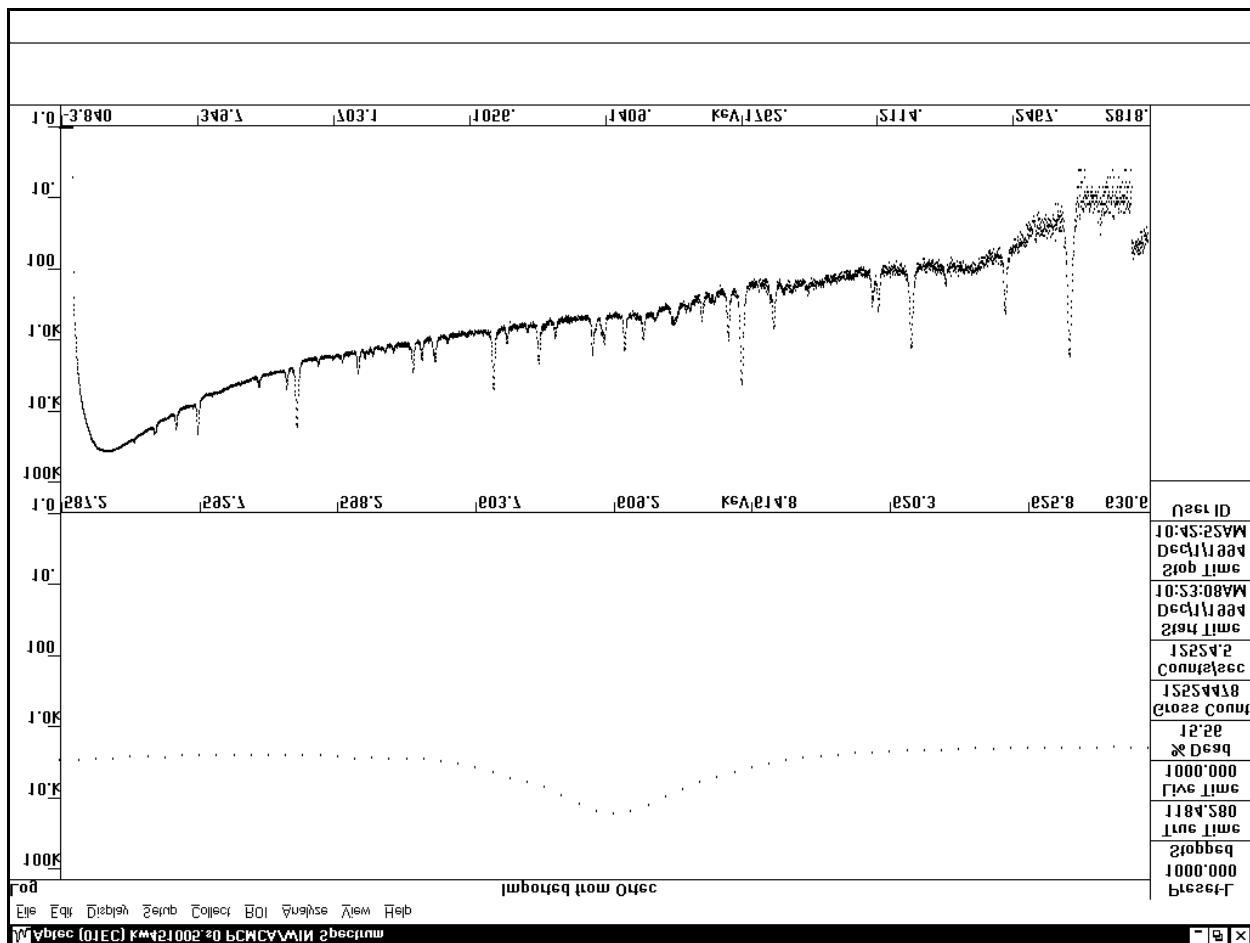


Figure 6-6. Spectrum from the KW Calibration Standard Recorded by Gamma 1A with Water in the Test Hole. The spectrum identification label is KW451005.S0, and the spectrum was recorded on December 1, 1994 during the base calibration. The upper half of the figure shows the magnified peak associated with the 609.3-keV gamma ray. The FWHM of this peak is 4.25 keV, which is much larger than the FWHM from the spectra recorded by Gamma 1B.

The peaks in the spectrum from the water-filled test hole are obviously distorted. The distortion of the 609.3-keV peak is illustrated in Figure 6-7.

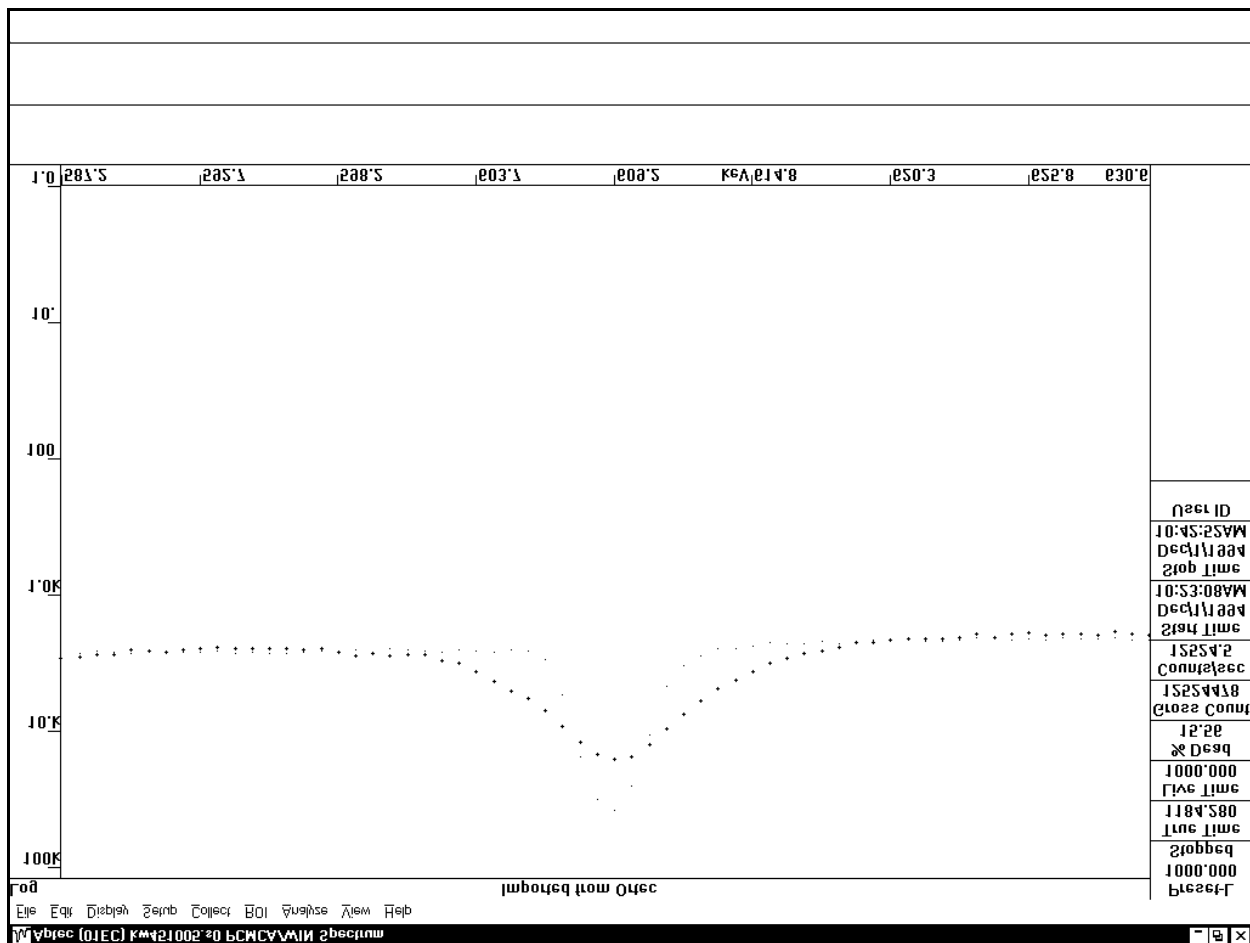


Figure 6-7. Magnified 609.3-keV Spectral Peaks from Spectrum SBMC005.S0 (Depicted by Small Symbols) and Spectrum KW451005.S0 (Depicted by Large Symbols).

Distortion of the peaks affects the peak intensity calculations. Peak intensities are normally calculated using the *multifit* feature in the spectrum analysis software. The *multifit* algorithm fits a Gaussian peak to the data, then calculates the area under the Gaussian peak. Symbols in Figure 6-8 show the 609.3-keV peak from spectrum SBMC005.S0. Vertical lines in the figure indicate the multichannel analyzer channels that span the peak, and the closely spaced dots depict the Gaussian peak that was fitted to the data by the spectrum analysis software. The horizontal line represents the background level that was determined by the spectrum analysis software. In this example, the data points are well represented by the Gaussian peak.

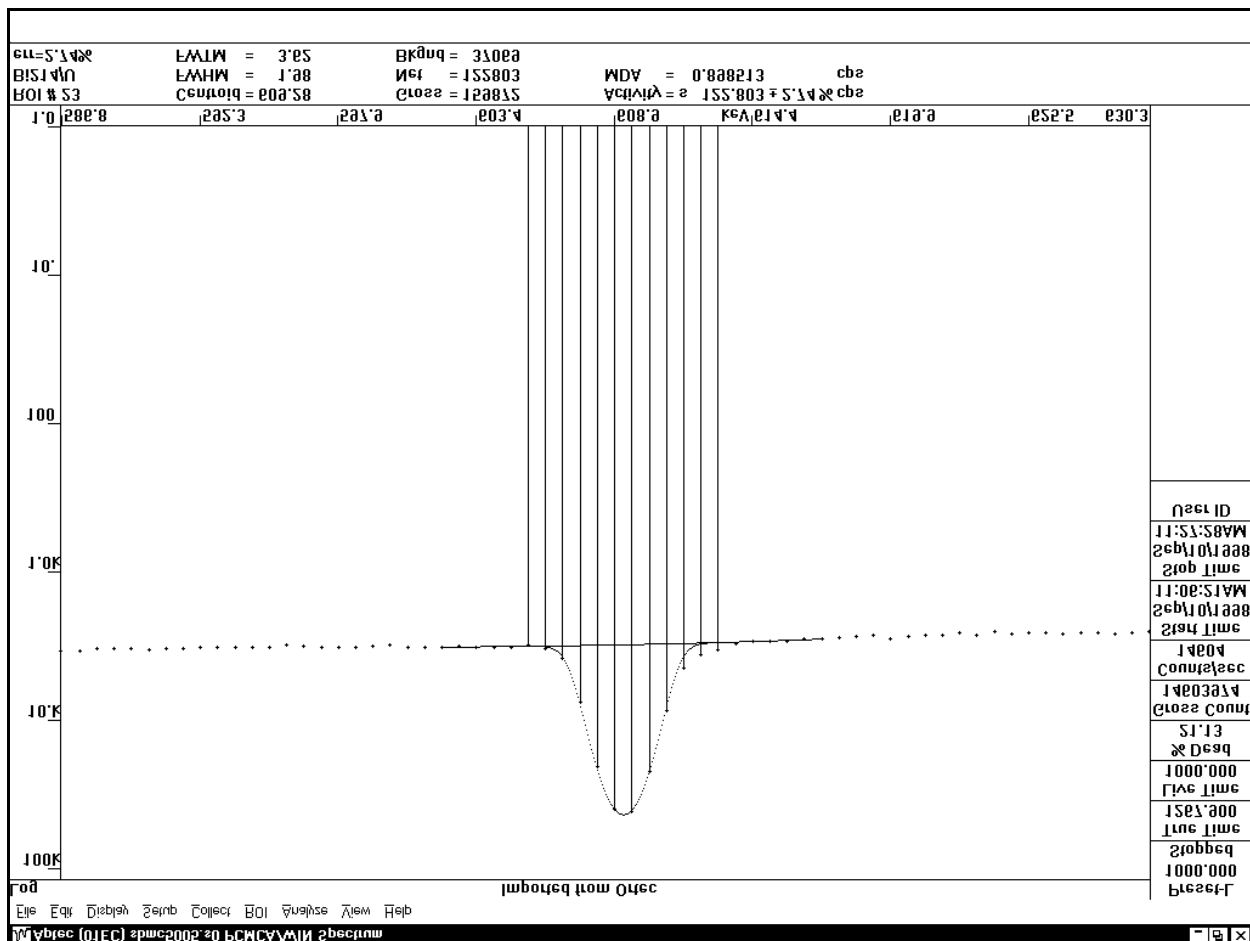


Figure 6-8. Magnified 609.3-keV Spectral Peak from Spectrum SBMC005.S0 (Symbols and Vertical Lines) with the Gaussian Fit Determined by Multifit (Closely Spaced Dots).

The 609.3-keV peak and the Gaussian fitted peak from spectrum KW451005.S0 are shown in Figure 6-9. For this distorted peak, the area under the Gaussian peak is obviously smaller than the actual peak area.

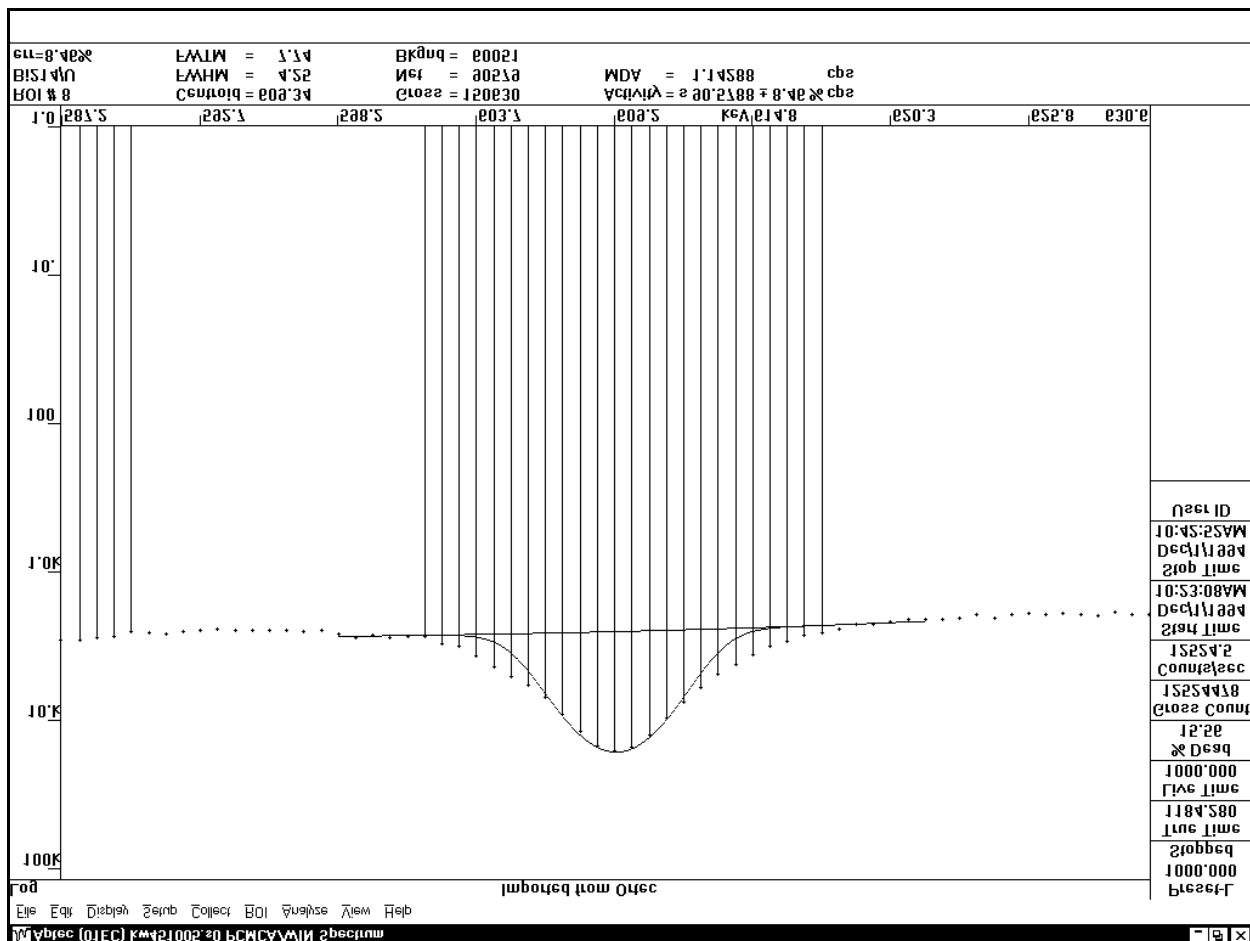


Figure 6-9. Magnified 609.3-keV Spectral Peak from Spectrum KW451005.S0 (Symbols and Vertical Lines) with the Gaussian Fit Determined by Multifit (Closely Spaced Dots).

All of the base calibration spectra recorded with the Gamma 1A sonde immersed in water displayed peak distortion, and the Gaussian fitted peaks consistently yielded intensities that were significantly smaller than the actual intensities. These observations prompted the following investigation.

The intensity (peak area) of the 609.3-keV peak shown in Figure 6-9 was  $90.6 \pm 7.7$  counts per second by the *multifit* (Gaussian fitting) calculation, but was  $108.4 \pm 1.2$  counts per second if calculated by the *peaksearch* algorithm. The *peaksearch* algorithm performs no Gaussian fitting, but simply sums the (background-subtracted) counts in the peak. Because the *multifit* calculations yielded peak intensities that were consistently too small, one might suspect that more accurate peak intensities would result if the *peaksearch* algorithm were used.

To check this hypothesis, the peak intensities for the water-filled-hole base calibration spectra were recalculated using the *peaksearch* algorithm. All of the peak intensities were higher than the intensities calculated with *multifit*, and the higher peak intensities led to lower water corrections. The recalculated water corrections are displayed, along with the corrections from the sixth recalibration data, in Figure 6-10.

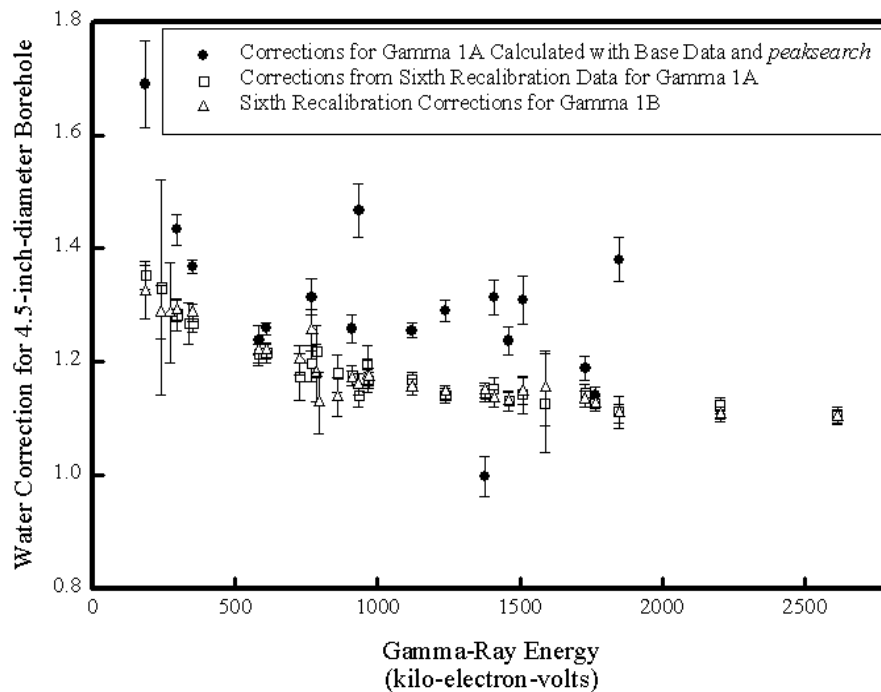


Figure 6-10. Gamma 1 Water Corrections Calculated with Peaksearch Data Compared to Corrections Calculated with Multifit Data

The plots in Figure 6-10 show the effect of recalculating the peak intensities in the Gamma 1A base calibration spectra from the water-filled test holes. The recalculated water corrections are consistently smaller than the original corrections, as expected, and are more consistent with the sixth recalibration corrections than the original corrections. The recalculated corrections do not appear to coincide with the sixth recalibration corrections, but this point is inconclusive because of the scatter in the recalculated corrections.

Because the distortion of peaks was not observed in any base calibration spectra recorded by Gamma 1A except the water-filled-hole spectra, it is nearly certain that an electrical malfunction in the Gamma 1A sonde afflicted the base calibration spectra that were collected when the sonde was immersed in water. The consequence of this electrical malfunction was severe degradation of the spectral peaks. Departure of the spectral peaks from the Gaussian shape caused the spectrum analysis program to calculate peak intensities that were consistently too small, and because these offsets appeared in the spectra from the water-filled test holes, but not in the spectra from the dry test holes, the water corrections calculated with Equation 6-2 were systematically high.

It is also apparent that the spectra acquired for the sixth recalibration with the Gamma 1A sonde immersed in water did not have distorted peaks. The electrical problem was apparently corrected



during one of the several repair sessions of the Gamma 1A sonde that took place over the duration of the logging program. Although no attempts were specifically made to isolate this particular Gamma 1A problem, the problem must have been inadvertently corrected when other repairs were undertaken.

Because water-filled-hole measurements were not routinely repeated at the periodic recalibrations, there is just one way to pinpoint the time at which the Gamma 1A electrical problem disappeared. Technical staff members would have to review the Gamma 1A repair records, then examine the Tank Farms data taken from water-filled boreholes before and after each repair. If the peak distortion was present before a particular repair, but not after, then that repair could be identified as the one that fixed the problem. However, such an effort is probably unnecessary for several reasons. First, although the Gamma 1A baseline corrections are offset from the corresponding corrections for Gamma 1B, Gamma 2A, and Gamma 2B, they are still correct for Gamma 1A data taken prior to the correction of the electrical problem as long as the peak intensities are calculated with *multifit* and not with *peaksearch*. Second, if the Gamma 1A baseline correction had been applied to data taken with Gamma 1A after the problem was corrected, the overcorrection by about 20 percent would have produced offsets (i.e., discontinuous jumps in concentration when the sonde passed from water to air) in the calculated concentrations that would have caught the data analysts' attention. Because no glaring overcorrections were noted, there is no reason to re-examine the old data.

However, the Gamma 1A baseline corrections are obviously incorrect if the electrical problem is fixed, so the water corrections appropriate for *future* data analysis must be determined. New water correction data cannot be easily recorded because the calibration standards at Hanford do not offer a range of test hole diameters. It is therefore recommended that the baseline water corrections for Gamma 2A be used in the future to process data collected from water-filled boreholes with Gamma 1A or Gamma 1B.

This recommendation is justified by the base calibration casing correction results for Gamma 1A and Gamma 2A. Like water in the borehole, casing presents an attenuating medium between the gamma-ray source in the formation and the gamma-ray detector, but all of the casing correction data were acquired without water in the test hole, and therefore, without the effect of the electrical problem on the Gamma 1A data. Figure 6-11 shows casing corrections for three casing thicknesses plotted in relation to gamma-ray energy. The corrections were calculated using the established casing correction equation, Equation (35) in DOE (1995b). These plots show that in all cases a correction for Gamma 2A is essentially identical to the analogous correction for Gamma 1A.

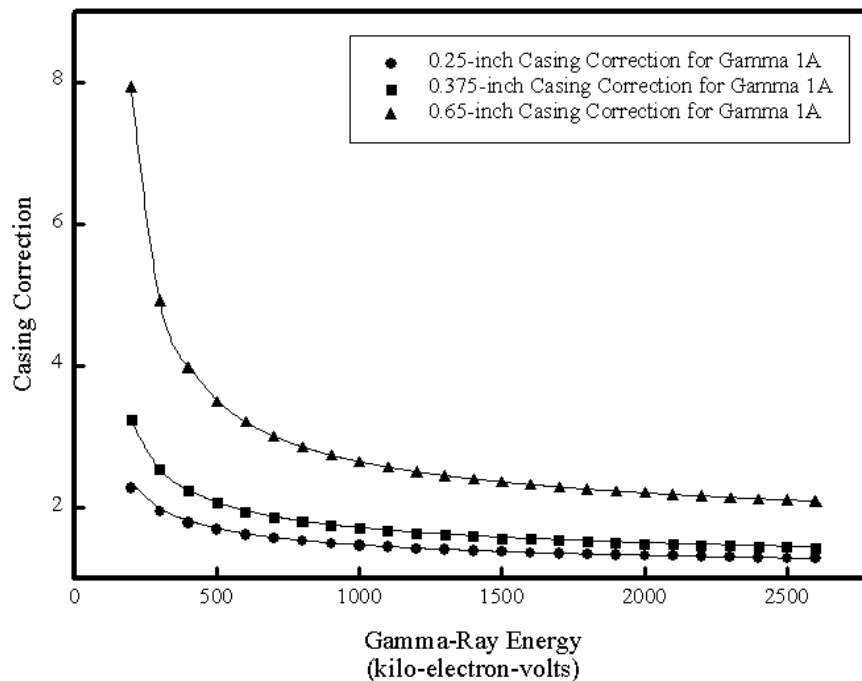


*Figure 6-11. Casing Corrections for Three Casing Thicknesses. Symbols show calculated corrections for Gamma 1A and solid lines represent the corresponding calculated corrections for Gamma 2A. Both sets of corrections were calculated using correction equations derived from the base calibration data.*

## **7.0 Acknowledgments**

The new acceptance tests and the tolerances for the field verifications were developed by Mr. Richard G. McCain.

This report was prepared for publication by Ms. Rachel Paxton.

## 8.0 References

Erdtmann, G., and W. Soyka, 1979. *The Gamma Rays of the Radionuclides*, Verlag Chemie, New York.

Friedlander, G., J.W. Kennedy, E.S. Macias, and J.M. Miller, 1981. *Nuclear and Radiochemistry* (Third Edition), John Wiley and Sons, Inc., New York.

Heistand, B.E., and E.F. Novak, 1984. *Parameter Assignments for Spectral Gamma-Ray Borehole Calibration Models*, GJBX-(284), prepared by Bendix Field Engineering Corporation for the U.S. Department of Energy Grand Junction Projects Office, Grand Junction, Colorado.

Leino, R., D.C. George, B.N. Key, L. Knight, and W.D. Steele, 1994. *Field Calibration Facilities for Environmental Measurement of Radium, Thorium, and Potassium*, DOE/ID/12584-179 GJ/TMC-01 (Third Edition) UC-902, prepared by RUST Geotech, Inc., for the U.S. Department of Energy Grand Junction Office, Grand Junction, Colorado.

Trahey, N.M., A.M. Voeks, and M.D. Soriano, 1982. *Grand Junction/New Brunswick Laboratory Interlaboratory Measurement Program: Part I -- Evaluation; Part II -- Methods Manual*, Report NBL-303, New Brunswick Laboratory, Argonne, Illinois.

U.S. Department of Energy (DOE), 1995a. *Vadose Zone Monitoring Project at the Hanford Tank Farms Spectral Gamma-Ray Borehole Geophysical Logging Characterization and Baseline Monitoring Plan for the Hanford Single-Shell Tanks* (Rev. 0), P-GJPO-1786, prepared by Rust Geotech for the U.S. Department of Energy Grand Junction Office, Grand Junction, Colorado.

\_\_\_\_\_, 1995b. *Vadose Zone Monitoring Project at the Hanford Tank Farms Calibration of Two Spectral Gamma-Ray Logging Systems for Baseline Characterization Measurements in the Hanford Tank Farms* (Rev. 0), GJPO-HAN-1, prepared by Rust Geotech for the U.S. Department of Energy Grand Junction Office, Grand Junction, Colorado.

\_\_\_\_\_, 1996a. *Vadose Zone Characterization Project at the Hanford Tank Farms, Biannual Recalibration of Two Spectral Gamma-Ray Logging Systems Used for Baseline Characterization Measurements in the Hanford Tank Farms* (Rev. 0), DOE/ID/12584-266 GJPO-HAN-3, prepared by Rust Geotech for the U.S. Department of Energy Grand Junction Office, Grand Junction, Colorado.

\_\_\_\_\_, 1996b. *Vadose Zone Characterization Project at the Hanford Tank Farms, Second Biannual Recalibration of Two Spectral Gamma-Ray Logging Systems Used for Baseline Characterization Measurements in the Hanford Tank Farms* (Rev. 0), DOE/ID/12584-281 GJPO-HAN-5, prepared by Rust Geotech for the U.S. Department of Energy Grand Junction Office, Grand Junction, Colorado.

U.S. Department of Energy (DOE), 1997. *Hanford Tank Farms Vadose Zone, Third Biannual Recalibration of Two Spectral Gamma-Ray Logging Systems Used for Baseline Characterization Measurements in the Hanford Tank Farms* (Rev. 0), GJO-97-22-TAR GJO-HAN-13, prepared by MACTEC-ERS for the U.S. Department of Energy Grand Junction Office, Grand Junction, Colorado.

\_\_\_\_\_, 1998a. *Hanford Tank Farms Vadose Zone, Fourth Biannual Recalibration of Spectral Gamma-Ray Logging Systems Used for Baseline Characterization Measurements in the Hanford Tank Farms* (Rev. 0), GJO-97-23-TAR GJO-HAN-14, prepared by MACTEC-ERS for the U.S. Department of Energy Grand Junction Office, Grand Junction, Colorado.

\_\_\_\_\_, 1998b. *Hanford Tank Farms Vadose Zone, Fifth Biannual Recalibration of Spectral Gamma-Ray Logging Systems Used for Baseline Characterization Measurements in the Hanford Tank Farms* (Rev. 0), GJO-98-41-TAR GJO-HAN-20, prepared by MACTEC-ERS for the U.S. Department of Energy Grand Junction Office, Grand Junction, Colorado.

Wilson, R.D., and D.C. Stromswold, 1981. *Spectral Gamma-Ray Logging Studies*, GJBX-21(81), prepared by Bendix Field Engineering Corporation for the U.S. Department of Energy Grand Junction Projects Office, Grand Junction, Colorado.